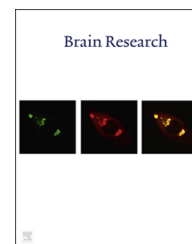


Available online at [www.sciencedirect.com](http://www.sciencedirect.com)
[www.elsevier.com/locate/brainres](http://www.elsevier.com/locate/brainres)

## Research Report

# Sensorimotor synchronization with tempo-changing auditory sequences: Modeling temporal adaptation and anticipation



M.C. (Marieke) van der Steen<sup>a,\*</sup>, Nori Jacoby<sup>b</sup>, Merle T. Fairhurst<sup>a</sup>,  
Peter E. Keller<sup>a,c</sup>

<sup>a</sup>Max Planck Research Group “Music Cognition and Action Group”, Max Planck Institute for Human Cognitive and Brain Sciences, PO Box 500355, 04303 Leipzig, Germany

<sup>b</sup>The Edmond and Lily Safra Center for Brain Sciences, Hebrew University, Jerusalem, Israel and Music Department, Bar Ilan University, Ramat Gan, Israel

<sup>c</sup>The MARCS Institute, University of Western Sydney, Sydney, NSW, Australia

### ARTICLE INFO

#### Article history:

Accepted 31 January 2015

Available online 25 February 2015

#### Keywords:

Sensorimotor synchronization

Temporal adaptation

Error correction

Temporal anticipation

Predictive internal models

Computational model

### ABSTRACT

The current study investigated the human ability to synchronize movements with event sequences containing continuous tempo changes. This capacity is evident, for example, in ensemble musicians who maintain precise interpersonal coordination while modulating the performance tempo for expressive purposes. Here we tested an ADaptation and Anticipation Model (ADAM) that was developed to account for such behavior by combining error correction processes (adaptation) with a predictive temporal extrapolation process (anticipation). While previous computational models of synchronization incorporate error correction, they do not account for prediction during tempo-changing behavior. The fit between behavioral data and computer simulations based on four versions of ADAM was assessed. These versions included a model with adaptation only, one in which adaptation and anticipation act in combination (error correction is applied on the basis of predicted tempo changes), and two models in which adaptation and anticipation were linked in a joint module that corrects for predicted discrepancies between the outcomes of adaptive and anticipatory processes. The behavioral experiment required participants to tap their finger in time with three auditory pacing sequences containing tempo changes that differed in the rate of change and the number of turning points. Behavioral results indicated that sensorimotor synchronization accuracy and precision, while generally high, decreased with increases in the rate of tempo change and number of turning points. Simulations and model-based parameter estimates showed that adaptation mechanisms alone could not fully explain the observed precision of sensorimotor synchronization. Including anticipation in the model increased the precision of simulated sensorimotor

Abbreviations: SMS, sensorimotor synchronization; IOI, inter-onset interval; ITI, inter-tap interval; PT-ratio, prediction/tracking ratio; PT-index, prediction/tracking index; ADAM, ADaptation and Anticipation Model; ANOVA, analysis of variance; bGLS, bounded Generalized Least Squares

\*Corresponding author.

E-mail address: [steen@cbs.mpg.de](mailto:steen@cbs.mpg.de) (M.C. van der Steen).

<http://dx.doi.org/10.1016/j.brainres.2015.01.053>

0006-8993/© 2015 Elsevier B.V. All rights reserved.

synchronization and improved the fit of model to behavioral data, especially when adaptation and anticipation mechanisms were linked via a joint module based on the notion of joint internal models. Overall results suggest that adaptation and anticipation mechanisms both play an important role during sensorimotor synchronization with tempo-changing sequences.

*This article is part of a Special Issue entitled SI: Prediction and Attention.*

© 2015 Elsevier B.V. All rights reserved.

## 1. Introduction

Music making often involves multiple performers collectively producing actions that vary in tempo. This purposeful non-stationarity in tempo, which plays a role in communicating musical expression to an audience, places challenges upon interpersonal coordination. Sometimes the composer specifies the manner in which the tempo should change by using terms such as ‘ritardando’ (slowing down gradually) and ‘accelerando’ (speeding up) in the musical notation. However, performers typically introduce additional planned or spontaneous tempo changes to convey their interpretation of a piece (e.g., Keller, 2014; Wing et al., 2014). Furthermore, tempo changes might arise unintentionally as a result of the relation between musical structure and patterns of performance expression (e.g., Repp, 1998, 2008; Repp and Bruttomesso, 2009) and as a result of the dynamic interplay between musicians (Palmer, 1997; Madison and Merker, 2005).

One of the underlying factors that contribute to successful interpersonal coordination is the timing of one’s actions with an external stimulus (e.g., the tones produced by a fellow musician) (Repp, 2005). Humans have the ability to synchronize their movements successfully even with complex timing sequences that contain tempo changes (Repp, 2002a; Rankin et al., 2009; Pecenka and Keller, 2011). Synchronizing actions with tempo-changing sequences is not only important in the music domain. In sports and daily life, people are required to synchronize their movements with sequential events at different rates and to handle rate changes, in order to fulfill task requirements successfully. An example is the Olympic rowing team that in the heat of the moment is instructed by the coxswain to speed up the pace in order to overtake a competing team. A daily life example occurs if you change pace while walking through the city together with a friend who suddenly speeds up in order to be able to cross the street before the light at the pedestrian crossing turns red. The current study investigates how people synchronize their movements with different types of ongoing tempo changes. Our main goal is to identify and gain a better understanding of the mechanisms that underlie this extraordinary form of sensorimotor synchronization skill.

Individuals’ sensorimotor synchronization (SMS) abilities and the underlying mechanisms are often investigated by means of paced finger-tapping tasks (Michon, 1967; Repp, 2005). During such tasks, participants are asked to tap with their finger in time with the events (e.g., tones) of computer-controlled pacing sequences. The instruction is typically to synchronize finger taps as accurately and precisely as possible with the stimulus sequence. The mean asynchrony between finger taps and

stimulus events can be used as an inverse measure of SMS accuracy, and the variability (i.e., standard deviation) of the asynchronies can serve an inverse measure of SMS precision. The pacing sequences are often isochronous series of tones, but sometimes timing perturbations (lengthened or shortened inter-onset intervals) are added. These perturbations can vary in terms of whether they are predictable or unpredictable and whether they are local (i.e., affecting one single event or interval) or global (i.e., affecting every event).

It has been hypothesized that in order to successfully time movements relative to external events, humans employ mechanisms that enable adaptation (reactive error correction) and anticipation (tempo-change prediction) (e.g., Keller, 2008; van der Steen and Keller, 2013). Temporal adaptation processes have been studied extensively in the tradition of information-processing approaches to SMS. According to the information-processing theory, the timing of simple movements is determined by an internal timekeeping process that generates pulses that, in turn, trigger motor responses (e.g., taps) (Wing and Kristofferson, 1973). The timekeeper outputs intervals of a particular duration (i.e., period) that may or may not change during synchronization. Variability in movement timing arises due to variance in this central timekeeper, and also as a result of variable transmission delays in the peripheral motor system (e.g., Vorberg and Wing, 1996).

Adaptation mechanisms reduce the effects of timing variability and therefore contribute to successful SMS (e.g., Mates, 1994a, 1994b; Vorberg and Wing, 1996). Two types of adaptation mechanisms – phase and period correction – have been distinguished (Mates, 1994a, 1994b; Vorberg and Wing, 1996; Semjen et al., 1998). Both error correction processes modify the timing of the next tap based on a proportion of the asynchrony, the timing error between a tap and stimulus event (Fig. 1). Phase correction is an automatic and local adjustment of the interval generated by the internal timekeeper, leaving the interval setting of this timekeeper unaffected (Repp, 2001a, 2002b) (Fig. 1A). Period correction on the other hand changes the interval setting of the timekeeper that drives the motor activity (Fig. 1B). This change in timekeeper setting persists until period correction is applied again (Repp, 2001b). Period correction requires the conscious perception of a tempo change in the stimulus sequence (Repp and Keller, 2004). Without these adaptation mechanisms, movement timing variability accumulates from movement cycle to movement cycle. This leads to increasingly large asynchronies, phase drift and eventually the loss of synchronization (Vorberg and Wing, 1996).

In addition to the adaptation mechanisms, it has been suggested that anticipation mechanisms contribute to successful

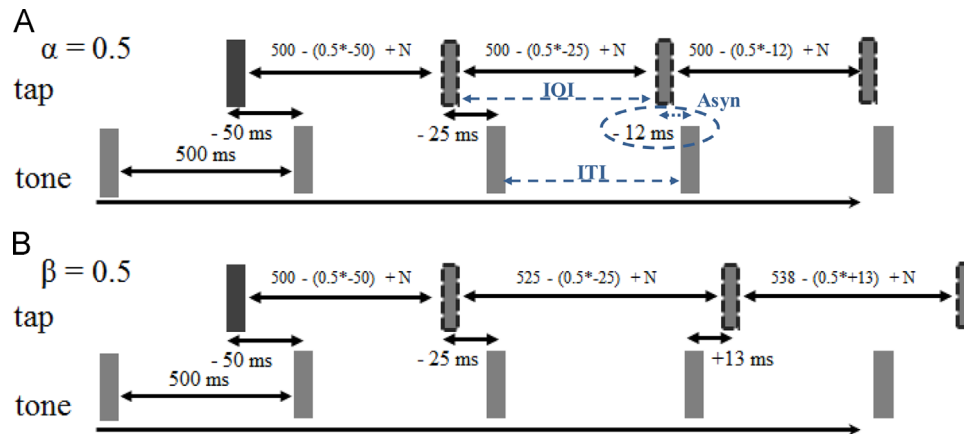


**Fig. 1 – Schematic representation of conventional SMS variables and the effects of phase and period correction.** Standard variables related to a paced finger-tapping task are depicted in blue and dashed. *Asyn* reflects the asynchrony (timing error) between the finger tap and the tone. *ITI* stands for inter-tap interval, the interval between two successive taps. *IOI* stands for inter-onset interval, the interval between two onsets of the stimulus sequence. Equations governing phase and period correction are:  $t_{n+1} = t_n + T_n - (\alpha + \beta) \times asyn_n + noise$  and  $T_{n+1} = T_n - \beta \times asyn_n$ . Where  $\alpha$  reflects the phase correction parameter and  $\beta$  the period correction parameter,  $t_n$  is the timing of the next tap, and  $T_n$  the current timekeeper setting (see Section 4). The timekeeper originally has an interval setting of 500 ms. Adapted from van der Steen and Keller (2013).

SMS, especially during SMS with tempo-changing sequences (Keller, 2008; van der Steen and Keller, 2013). Anticipation occurs when actions not only depend on the past and present but also on predictions, expectations, or beliefs about the future (Butz et al., 2003). Tempo-change predictive processes allow the anticipation of the precise time of onset of upcoming stimulus events. Based on the anticipated onsets, individuals can initiate their movements early enough to ensure that responses coincide with the upcoming events (Schmidt, 1968).

Behavioral evidence for tempo-change prediction during SMS is found in positive dependencies (lag-0 cross-correlations) between the inter-tap intervals (ITIs) and inter-onset intervals (IOIs) in tempo-changing sequences. The lag-0 cross-correlation can be compared with the lag-1 cross-correlation between ITIs and IOIs, which reflects the tendency to track, or copy, rather than to predict the IOIs during synchronization with the tempo changes. Previous work suggests that humans can engage in predictive and tracking behavior simultaneously (Repp, 2002a; Rankin et al., 2009). Pecenkova and Keller (2011) therefore used the ratio between the lag-0 and lag-1 cross-correlations of ITIs and IOIs as a measure of prediction in SMS with tempo-changing tapping tasks. A prediction/tracking ratio (PT-ratio) larger than 1 reflects the individual's tendency to predict ongoing tempo changes, while a ratio smaller than 1 indicates that the individual tends to track tempo changes by copying the most recent IOI. PT-ratios larger than 1 suggest the involvement of higher-order anticipation mechanisms involving temporal extrapolation based on at least two preceding IOIs. These mechanisms support temporal predictions and thus provide information about the direction of tempo change (speeding up/slowing down) in the pacing sequence.

Previous research has shown that asynchronies are reduced when individuals are able to predict upcoming timing perturbations under situations where tempo fluctuations are systematic and detectable (Michon, 1967; Repp, 2005).

Individuals who display relatively strong prediction tendencies (reflected in high PT-ratios) synchronize more precisely than individuals who tend to track tempo changes (Mills et al., in press; Pecenkova and Keller, 2009, 2011). In musical contexts, it has been shown that individuals anticipate tempo variations in familiar musical pieces and that synchronization performance improves as a result of learning patterns of tempo change (Repp, 2002a; Rankin et al., 2009). This type of higher-order anticipation appears to be effortful, as it has been found to be subject to interference by an attentionally demanding secondary task (Pecenkova et al., 2013).

Tracking behavior has been observed during synchronization tasks in which the stimulus sequence contains timing perturbations that are random or barely detectable (e.g., Thaut et al., 1998a, 1998b, 2009; Madison and Merker, 2005). Even pacing sequences that mirror the expressive timing profile of a musical performance (e.g., ritardando or accelerando) elicit tracking behavior when participants are unaware of the systematic changes (Repp, 2002a, 2006).

It has been proposed that the anticipatory mechanisms that support SMS with tempo-changing sequences recruit internal models in the central nervous system (Keller et al., 2007; Keller, 2008, 2012; van der Steen and Keller, 2013). This proposal is founded upon research in the field of computational movement neuroscience, where it has been theorized that anticipatory movement control is underpinned by internal models that represent bi-directional ('forward' and 'inverse') transformations between movements and their sensory effects (see e.g., Wolpert et al., 2003). Forward models represent the causal relationship between the input and output of the action control system and are thereby able to predict the effect of a given motor command on the body and the environment. Inverse models serve as a controller for intentional movements by providing motor commands that are potentially able to change the current state of the body

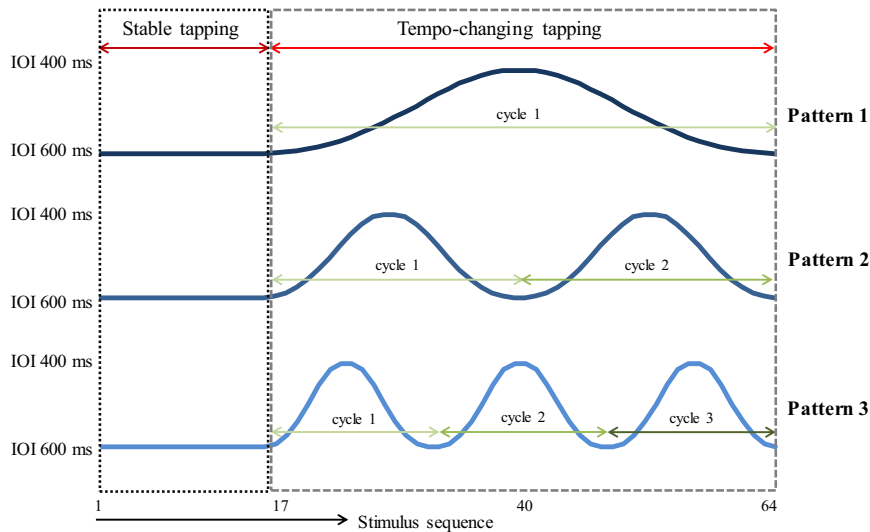


**Fig. 2 – The three tempo-changing patterns.** Each trial started with four initiation tones with an IOI of 600 ms. The stimulus sequences consisted of 64 tones. The tempo of the first 16 tones was stable (IOI 600 ms) [black dotted box], allowing synchrony to be established. The tempo during the following 48 tones varied between 600 and 400 ms IOI, following three sigmoidal patterns that resembled musical *accelerando* and *ritardando*. Data analyses focus on the tempo-changing part of the trials [gray dashed box] (see Section 4).

and the environment to the desired end state. Paired inverse and forward models facilitate online motor control by allowing potential movement errors to be corrected before they occur (Wolpert and Kawato, 1998).

In the social domain, it has been claimed that internal models of one's 'own' actions operate in tandem with models that simulate the actions of 'others' (e.g., a stimulus event or another person) (Wolpert et al., 2003) to support joint action (Keller, 2008; Sebanz and Knoblich, 2009). Individuals may thus draw on their own sensory and motor systems to run internal models that simulate observed actions performed by others, thereby allowing the individual to predict others' action outcomes in terms of variety of features including timing (e.g., Grush, 2004; Pickering and Garrod, 2013, 2014; Wilson and Knoblich, 2005). It has, furthermore, been claimed that the coupling of 'own' and 'other' internal models in a 'joint' model facilitates sensorimotor synchronization by allowing the action control system to foresee potential errors in timing (asynchronies) and to correct these errors before they occur (van der Steen and Keller, 2013; Keller et al., 2014). A 'joint' internal model thus integrates outputs from 'own' and 'other' internal models. Based on discrepancies between these outputs, one's own actions can be modified to compensate in advance for any potential errors (Keller et al., in press).

Traditionally, adaptation and anticipation mechanisms have been investigated using separate paradigms. The ADaptation and Anticipation Model – ADAM – (van der Steen and Keller, 2013) was proposed as a unified framework to investigate the relationship between adaptation and anticipation. The core architecture of ADAM comprises three modules, one that governs adaptive timing (reactive error correction), another governing temporal anticipation (tempo-change prediction), and the final joint module linking the adaptation and anticipation modules. (The formal model architecture is described in detail in Section 4.2).

The adaptation module of ADAM determines the provisional timing of the next planned movement by implementing phase and period correction, which compensate for a proportion of each asynchrony between a movement and pacing sequence event. ADAM's anticipation module generates predictions about the timing of upcoming synchronization targets based the weighted sum of two processes, one entailing linear extrapolation of previous intervals in the pacing sequence and the other copying the previous interval. The linear extrapolation process is achieved via curve fitting that extends systematic patterns of tempo changes, such that a decelerating sequence with intervals that increase in duration will lead to a prediction that the next event will occur after an even longer interval, and vice versa for tempo accelerations. Finally, ADAM's joint module takes the outputs of the adaptation module (the provisional time of the next planned movement) and the anticipation module (the next predicted tone onset time) and computes the discrepancy between them. An anticipatory error correction process then compensates for a proportion of this discrepancy, and (if necessary) the timing of the next movement is modified accordingly.

One of the goals in developing ADAM was to provide a unified platform upon which adaptation and anticipation mechanisms, and possible links between these mechanisms, can be systematically explored by means of computer simulations and their relation to behavioral data. The current study pursued this aim with a view to understanding how individuals synchronize their movements with sequences containing continuous tempo changes. Specific goals were to investigate how adaptation and anticipation mechanisms contribute to successful SMS behavior with tempo-changing sequences, and to test the hypothesis that joint internal models play a role in linking adaptation and anticipation mechanisms. To this end, data from a behavioral experiment are compared against ADAM simulations with different combinations of modules.

In the behavioral experiment, participants tapped their finger in synchrony with three auditory sequences that differed in the rate of tempo change and the number of turning points (Fig. 2). We employed three different tempo-changing stimulus sequences to test whether the contributions of adaptation and anticipation mechanisms vary as a function of the rate of tempo change and frequency of tempo reversals (which may affect the amount of overshoot at turning points). After a section in which the tempo was stable (to allow synchronization to be easily established), the tempo of the stimulus sequences varied between 600 and 400 ms IOI. The difference between two successive IOIs ranged between 1 and 14 ms for pattern 1, between 4 and 28 ms for pattern 2, and between 10 and 44 ms for pattern 3, the rate of tempo change thus increased from pattern 1 to 3. Pattern 1 had one cycle of acceleration followed by deceleration, pattern 2 had two cycles, and pattern 3 had three cycles (all within the same total duration). The tempo changes followed sigmoidal patterns that resembled musical *accelerando* and *ritardando* (Schulze et al., 2005).

Conventional synchronization measures related to the asynchrony between the participants' taps and the tones were employed as indices of SMS accuracy (mean asynchrony) and precision (standard deviation of asynchronies). Phase and period correction estimates were obtained by means of the bounded Generalized Least Squares (bGLS) as indicators of adaptation (Jacoby et al., in press; Jacoby and Repp, 2012). Two approaches were used to measure tempo-change prediction, the lagged cross-correlation method, yielding the PT-ratio (as described above; cf., Pecenka and Keller, 2009, 2011), and an alternative method that partials out autocorrelation from the time series by implementing pre-whitening and auto-regressive modeling (Mills et al., in press). The latter method yields a prediction/tracking index (PT-index), which reflects relatively strong temporal extrapolation when greater than 0 and relatively strong tracking when less than 0.

Computer simulations were run with ADAM to determine the effect of different combinations of mechanisms (instantiated as different modules in ADAM) on SMS precision. We employed four versions of ADAM: a model that only included adaptation, one in which adaptation and anticipation mechanisms interact indirectly (error correction related to the each asynchrony is applied to the next predicted IOI instead of the current timekeeper period), and two models in which adaptation and anticipation were linked directly in a joint module (with anticipatory error correction based on the discrepancy between outputs of the adaptation and anticipation module). The optimal usage of adaptation and anticipation mechanisms for successfully fulfilling the task instructions was ascertained by measuring the effect of varying parameter settings (i.e., the amount of phase/period correction, amount of temporal extrapolation/tracking, and the amount of anticipatory error correction) on simulated SMS precision (see Section 4).

In order to compare the behavioral data with the simulated results, we obtained parameter estimates for the four version of ADAM by means of the bGLS-method, and then calculated the fit of each model to the behavioral data. The fit of the models to the behavioral data is determined by calculating the log likelihood. Since our data contain a

relatively large number of samples, the log likelihood in this case is closely linked (identical numerically up to a small correction constant) to the AICc or the BIC criteria that had been substantiated in the literature for model comparison (Brockwell and Davis, 2009). For the simulations and model fitting, we focus on SMS precision as the dependent variable because in a previous study adaptation mechanisms were found to contribute more to SMS accuracy (mean asynchrony), while both adaptation and anticipation mechanisms contributed to SMS precision (standard deviation of asynchronies of asynchronies) (Mills et al., in press).

Our hypotheses address how the underlying adaptation and anticipation mechanisms are employed to achieve successful SMS with tempo-changing sequences. Based on previous studies that investigated the mechanisms separately, we hypothesize participants will generally show evidence for active adaptation and tempo-change prediction when synchronizing with the tempo-changing sequences (e.g., Repp, 2005; Pecenka and Keller, 2009, 2011). Accordingly, simulations and the fit of the different versions of ADAM should favor a synchronization model that includes both adaptation and anticipation mechanisms. Furthermore, models including the joint module should facilitate SMS behavior by allowing potential asynchronies to be corrected before they occur as a result of applying anticipatory error correction to compensate for discrepancies between adaptation and anticipation processes.

With respect to the three tempo-changing stimulus sequences, we expect that adaptation and anticipation will be affected by the rate of tempo change and frequency of turning points. We hypothesize that period correction will increase with the step size of the continuous tempo changes and that due to the automatic nature of phase correction these estimates remain constant. Finally, we assume that tempo-change prediction is more beneficial during the acceleration or deceleration phases of the tempo changes than at the transition between these phases, which are difficult to predict. We therefore hypothesize that an increasing number of transitions in the tempo-changing stimulus sequence will decrease SMS accuracy and precision.

---

## 2. Results

We first report behavioral data for SMS accuracy and precision, followed by estimates of adaptation (phase and period correction) and anticipation (PT-ratio & PT-index) derived from these data. Then we describe the results of computer simulations conducted with ADAM and, finally, the fit of different versions of ADAM to the behavioral data is reported.

### 2.1. Experiment

#### 2.1.1. Synchronization measures

Differences in synchronization accuracy and precision across the three tempo-changing patterns were investigated by examining the mean asynchrony and the standard deviation (SD) of asynchronies between participants' taps and pacing sequence tones. The results, averaged across participants, are displayed in Fig. 3. Separate repeated measures ANOVAs with pattern (1, 2, 3) as a within subject variable were performed

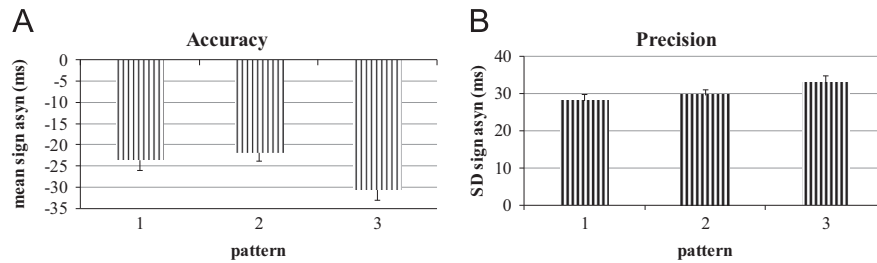


**Fig. 3 – The mean signed asynchrony as a measure of SMS accuracy (A) and the standard deviation of the signed asynchrony as a measure of SMS precision (B) for the three patterns. Error bars represent standard error across participants.**

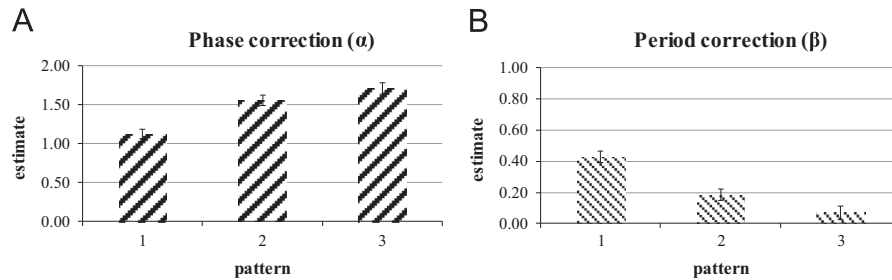


**Fig. 4 – Estimated amount of phase (A) and period (B) correction reflecting adaptation mechanisms. Error bars represent standard error across participants.**

on the mean asynchrony (accuracy) and the SD of asynchrony (precision) data.

The ANOVA on mean asynchrony yielded a significant main effect of pattern [ $F_{(2,32)}=15.67$ ,  $p<0.001$ ,  $\eta^2=0.14$ ]. Post-hoc pairwise comparisons [all  $p<0.01$ ] revealed that SMS accuracy was lower for pattern 3 (which had the highest rate of tempo change) compared to patterns 1 and 2 [all  $p<0.01$ ], while there was no significant difference in accuracy between patterns 1 and 2 (Fig. 3A). A significant main effect of pattern was also found for the standard deviation of asynchronies [ $F_{(2,32)}=7.34$ ,  $p<0.005$ ],  $\eta^2=0.08$ ]. Pairwise comparisons confirmed that SMS was less precise for pattern 3 compared to pattern 1 and 2 [all  $p<0.05$ ] (Fig. 3B), while differences between patterns 1 and 2 were non significant. This suggests that the high rate of tempo change in pattern 3 was especially challenging for participants to keep up with.

### 2.1.2. Adaptation measures

The amount of phase and period correction implemented by participants was estimated by means of the bGLS method using the ‘Adaptation Model’. Average estimates are displayed in Fig. 4. We performed a repeated measures ANOVA with correction type (phase/period) and pattern (1, 2, 3) as within-subject variables and the estimates as the dependent variable.

The ANOVA revealed significant main effects of correction type [ $F_{(1,16)}=368.17$ ,  $p<0.001$ ,  $\eta^2=0.89$ ] and pattern [ $F_{(2,32)}=5.50$ ,  $p<0.01$ ,  $\eta^2=0.05$ ]. The effect of correction type indicated that phase correction estimates were generally higher than period correction estimates. The effect of pattern was qualified by a significant interaction between pattern and correction type [ $F_{(2,32)}=57.41$ ,  $p<0.001$ ,  $\eta^2=0.46$ ], reflecting the fact that phase correction estimates increased while the period correction estimates decreased as the frequency of

tempo-change transitions increased from pattern 1 to 3. This interaction was explored further by analyzing the estimates for phase and period correction separately. A significant main effect of pattern was found for phase correction estimates [ $F_{(2,32)}=40.02$ ,  $p<0.001$ ,  $\eta^2=0.47$ ]. Pairwise comparisons revealed that phase correction estimates for pattern 1 were lower than for pattern 2 and 3 [all  $p<0.001$ ], while patterns 2 and 3 did not differ significantly (Fig. 4A). A significant main effect of pattern was also found for period correction estimates [ $F_{(2,32)}=29.12$ ,  $p<0.001$ ,  $\eta^2=0.48$ ]. Pairwise comparisons revealed that period correction estimates for pattern 1 was higher than for pattern 2 and 3 [all  $p<0.001$ ] and pattern 2 was higher than pattern 3 [ $p<0.05$ ] (Fig. 4B).

### 2.1.3. Anticipation measures

Anticipation mechanisms were investigated by examining the lag-0, lag-1 cross-correlations, the PT-ratio and the PT-index. These measures, averaged across participants, are displayed in Fig. 5. The repeated measures ANOVAs included pattern (1, 2, 3) and, if applicable, lag (0 or 1) as within subject variables. Furthermore, Pearson’s correlations between the PT-ratio and the PT-index were calculated separately for the three patterns across participants to assess the degree to which the two measures reflect similar processes.

The ANOVA on cross-correlation coefficients yielded significant main effects of pattern [ $F_{(2,32)}=59.94$ ,  $p<0.001$ ,  $\eta^2=0.43$ ] and lag [ $F_{(1,16)}=286.80$ ,  $p<0.001$ ,  $\eta^2=0.45$ ]. Pairwise comparisons revealed that cross-correlations were generally lower for pattern 3 compared to pattern 1 and 2, and for pattern 2 compared to pattern 1. Furthermore, the lag-0 cross-correlation was found to be higher than the lag-1 cross-correlation, which suggests a stronger tendency for tempo-change prediction than tracking (consistent with the PT-ratios, reported below). The interaction between pattern

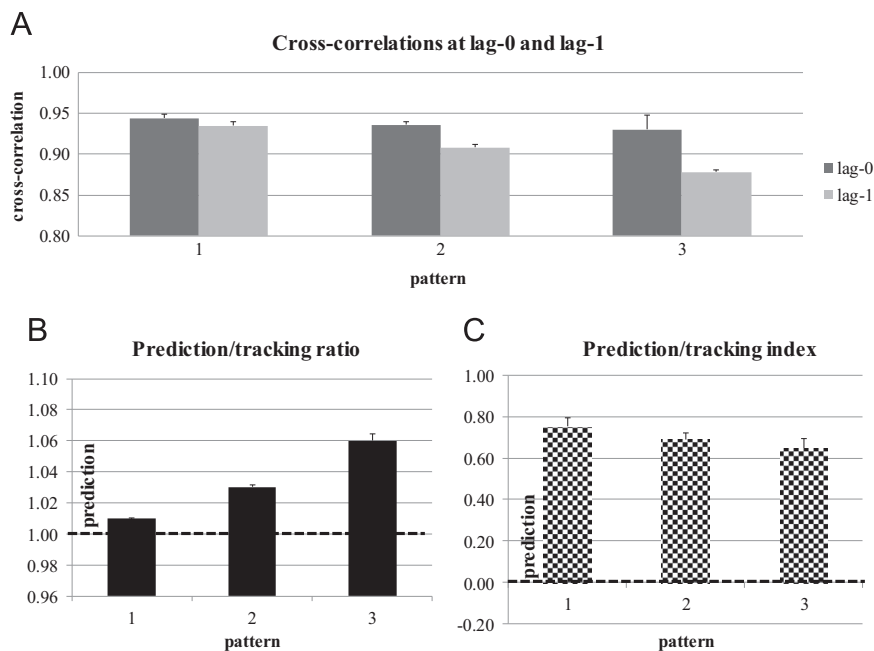


**Fig. 5 – The cross-correlations at lag-0 and lag-1(A), PT-ratio (B), and PT-index (C) reflecting anticipation. PT-ratios greater than 1 and PT-indices greater than 0 indicate that participants are predicting the tempo changes. Error bars represent standard error across participants.**

and lag also turned out to be significant for the cross-correlations [ $F_{(1.13,18.03)}=108.08$ ,  $p<0.001$ ,  $\eta^2=0.23$ ], as pattern had a stronger effect on lag-1 than lag-0 cross-correlation (Fig. 5A).

As implied by the main effect of lag reported above, PT-ratios for all patterns were greater than 1, suggesting that participants were predicting the tempo changes (Fig. 5B). The ANOVA on PT-ratios yielded a significant effect of pattern [ $F_{(1.11,17.79)}=107.51$ ,  $p<0.001$ ,  $\eta^2=0.77$ ]. Pairwise comparisons revealed that the PT-ratio was higher for pattern 3 compared to pattern 1 and 2, and that the PT-ratio was higher for pattern 2 than for pattern 1 [all  $p<0.001$ ].

All PT-indices (our alternative measure of prediction) were positive indicating that, also according to the auto-regression method, participants were predicting the tempo changes in the stimulus sequences (Fig. 5C). The result is important because it implies that the evidence for tempo-change prediction revealed in PT-ratios was not merely a consequence similar autocorrelation structures in IOI and ITI time series. The ANOVA on PT-indices yielded a significant effect of pattern [ $F_{(2,32)}=4.15$ ,  $p<0.05$ ,  $\eta^2=0.06$ ], reflecting a decrease in PT-indices (suggesting less prediction) from pattern 1 to pattern 3. This effect goes in the opposite direction to the effect found for PT-ratios (also note that the effect size is much smaller for PT-indices than PT-ratios), most likely due to differing degrees of autocorrelation in the patterns. Despite the opposite direction, the two measures were positively correlated across participants at the level of each pattern. Pearson's correlations between PT-ratio and PT-index were  $r=0.69$ ,  $0.94$ , and  $0.99$  for pattern 1, 2, and 3, respectively [all  $p<0.001$ ]. Thus, there was a moderately strong correlation between both measures for pattern 1 and a strong correlation for patterns 2 and 3.

## 2.2. Simulations

The results of simulations using the four versions of ADAM are shown in Fig. 6. This figure shows heat-maps of the SD of the signed asynchronies resulting from simulations across the parameter settings for the 'Adaptation Model' (A), 'Hybrid ADAM' model (B) 'Joint ADAM ( $\alpha$ )' model (C), and 'Joint ADAM ( $\beta$ )' model (D). Dark blue represents the highest SMS precision (low standard deviation of asynchronies), while the lowest SMS precision is presented in dark red. Extreme values (larger than three times the mean of the medians of the simulated SD of asynchronies) were replaced by the mean of the median for presentation purposes.

For the three tempo-changing synchronization patterns, the 'Adaptation model' (Fig. 6A) performed optimally (in terms of minimizing the SD of asynchronies) when a moderate amount of phase correction ( $\alpha$ ) and a moderate to high amount of period correction ( $\beta$ ) were employed. In Fig. 6A, across patterns, the dark blue shading shifts from the center to the right as period correction values increase along horizontal axis. This indicates that the standard deviation of asynchronies was lower, i.e., SMS precision was higher, especially when the model implemented higher levels of  $\beta$  when the rate of tempo change and number of turning points were high (pattern 2 and 3 compared to pattern 1). It can also be noted that several combinations of parameters, especially border parameters (e.g.,  $\alpha>1$  in combination with larger  $\beta$ ), led to extremely large and variable asynchronies due to drift. If the mean phase and period correction estimates of the participants (white boxes in Fig. 6A) are compared with the results of the simulations with the adaptation model, we find a simulated SMS precision of 32.35 ms for pattern 1, 55.05 ms for pattern 2, and 57.48 ms for pattern 3. It is noteworthy that participants were observed to be more precise than these

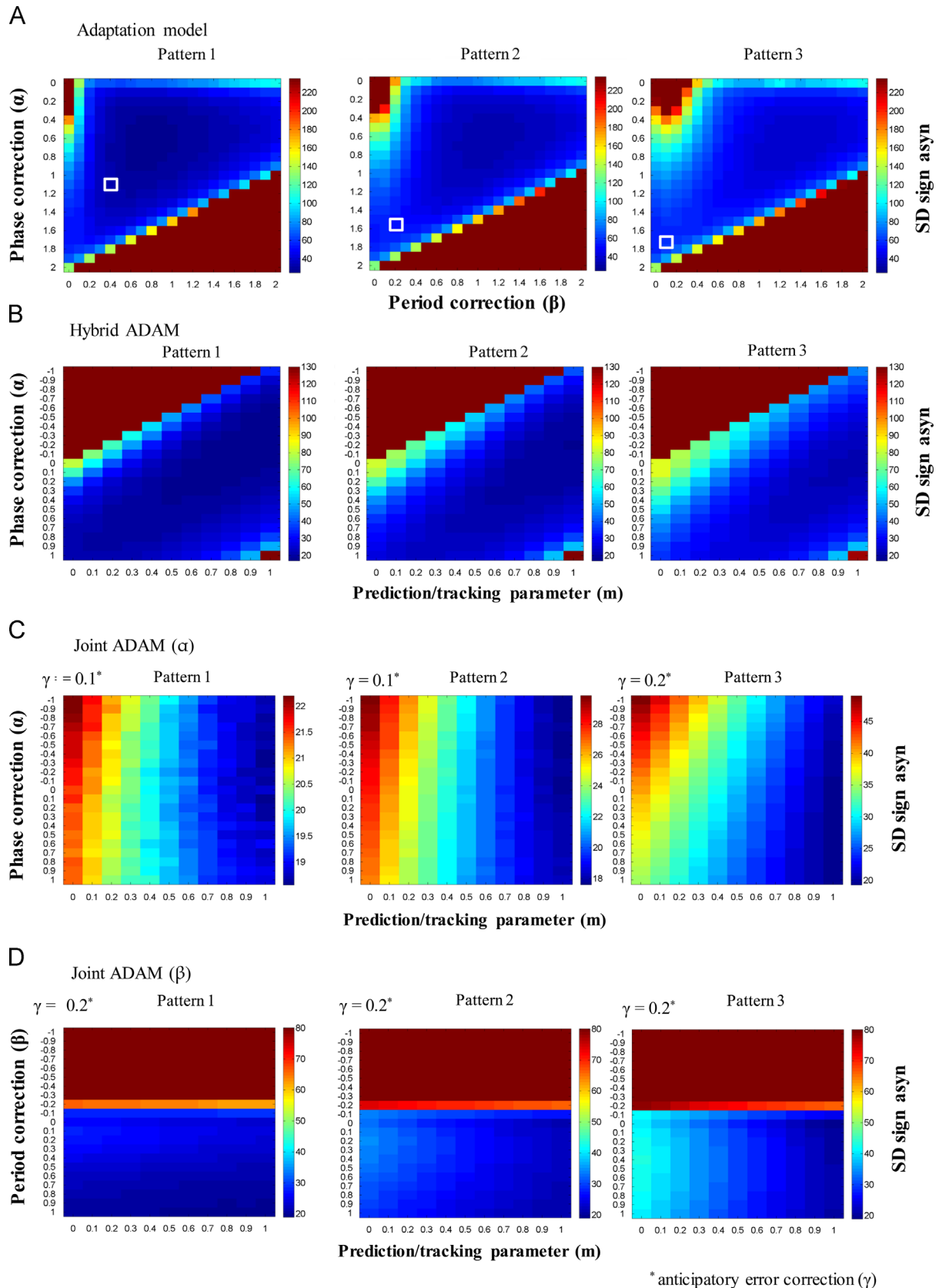


**Fig. 6 – Heat-maps showing the SD of the signed asynchronies resulting from simulations across the parameter settings for the ‘Adaptation Model’ (A), ‘Hybrid ADAM’ model (B) ‘Joint ADAM ( $\alpha$ )’ model (C), and ‘Joint ADAM ( $\beta$ )’ model (D). Dark blue represents the highest SMS precision (low standard deviation of asynchronies). Extreme values (larger than three times the mean of the medians of the simulated standard deviation of asynchronies) were replaced for presentation purposes. The white boxes in panel A reflect the mean phase and period estimates for the participants from the behavioral experiment.**

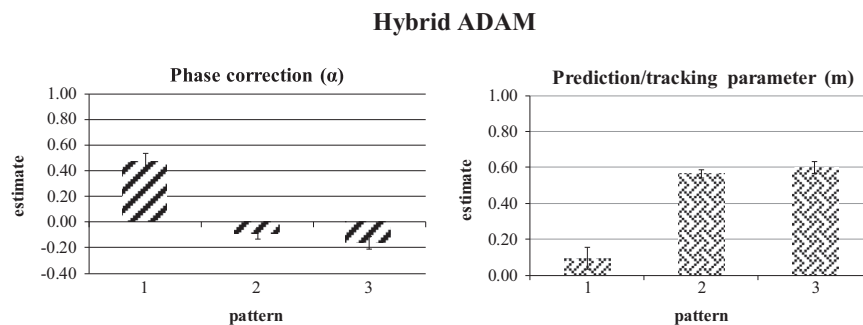


**Fig. 7 – Parameter estimates based on the ‘Hybrid ADAM’ model. Where  $\alpha$  reflects a phase correction parameter, while  $m$  indicates the prediction/tracking parameter. Error bars represent standard error across participants.**

simulated values particularly for patterns 2 and 3 (Fig. 3B), suggesting that adaptation mechanisms alone cannot account for all aspects of SMS behavior when the rate of tempo change is high.

The ‘Hybrid ADAM’ and ‘Joint ADAM ( $\alpha/\beta$ )’ models included adaptation and anticipation mechanisms. Anticipation is reflected in the prediction/tracking parameter  $m$ , which ranges from 0 to 1. The effect of this parameter is based on the assumption that humans engage in tempo-change prediction (i.e., tempo-change extrapolation based on the previous two IOIs) and tracking (copying the previous IOI) at the same time (Pecenka and Keller, 2011). The closer  $m$  is to 1, the more prediction takes place (i.e., tempo-change prediction based on the previous two IOIs). When  $m=0.5$  the model relies equal on prediction and tracking behavior to determine the timing of the next tone. An  $m$  smaller than 0.5 indicates that the model relies on tracking more than prediction.

Adaptation in the ‘Hybrid ADAM’ model is restricted to phase correction. As can be seen in Fig. 6B, negative phase correction settings ( $\alpha$ ) resulted in high variability of asynchronies due to drift (dark red in Fig. 6B). The simulation results illustrate that SMS precision increased with increases in the degree to which the models relied on prediction [higher  $m$ ] to determine the timing of the next tone. Specifically, lower SD asynchronies were found when  $m$  was greater than 0.5, reflecting the effect of prediction. Furthermore, when  $m$  was low, employing more phase correction has a beneficial effect on SMS precision (dark blue Fig. 6B).

In the ‘Joint ADAM ( $\alpha/\beta$ )’ models, adaptation and anticipation mechanisms were linked in a joint module that implements an anticipatory error correction process ( $\gamma$ ). This process uses the output of the adaptation module (planned tap time) and anticipation module (extrapolated tone time) to simulate what asynchrony would occur if the planned tap were to be produced, and then corrects for this anticipated error by the proportion  $\gamma$ . For the ‘Joint ADAM ( $\alpha/\beta$ )’ models, Fig. 6(C and D) shows the effect of  $m$  in the anticipation module and the error correction component ( $\alpha/\beta$ ) in the adaptation module for the mean  $\gamma$  estimate obtained via parameter estimation using the behavioral data (see below). Simulations indicated that relying more on tempo-change prediction had a positive effect on SMS precision. Lower SD asynchronies were observed with a higher prediction/tracking parameter  $m$  (dark blue Fig. 6C and D). The closer this parameter is to 1, the more the model relies on prediction.

Negative period correction ( $\beta$ ) settings in the adaptation module had a deteriorating effect on SMS precision, with settings beyond  $-0.2$  resulting in large variability (dark red in Fig. 6D).

### 2.3. Evaluation of the models

The four versions of ADAM were evaluated by estimating parameters from the behavioral data and then assessing the fit of each model to the behavioral data based on the log likelihood.

#### 2.3.1. Parameter estimates

Model parameters for the ‘Hybrid ADAM’ and ‘Joint ADAM ( $\alpha/\beta$ )’ models were estimated from the behavioral data by means of the bGLS-method. Estimates for the ‘Adaptation’ model were already presented in Section 2.1.2 and Fig. 3. For each parameter type, a separate repeated measures ANOVA with pattern (1, 2, 3) as the within subject variable was performed.

The ANOVAs on estimates from the ‘Hybrid ADAM’ model yielded significant main effects of pattern for  $\alpha$  [ $F_{(1.35,21.60)}=78.03$ ,  $p<0.001$ ] and  $m$  estimates [ $F_{(1.32,21.11)}=69.02$ ,  $p<0.001$ ]. Pairwise comparisons revealed that  $\alpha$  and  $m$  estimates for pattern 1 differed from estimates for pattern 2 and 3 (all  $p<0.001$ ), while pattern 2 and 3 estimates did not differ significantly. Specifically, for pattern 1, estimates of  $m$  were low (indicating tracking), while  $\alpha$ -estimates were high (phase correction). For pattern 2 and 3, when tempo changes are bigger, estimates of  $m$  were high (indicating prediction) and  $\alpha$  estimates were negative (suggesting correction in opposite direction) (Fig. 7).

For the ‘Joint ADAM ( $\alpha$ )’ model<sup>1</sup>, the ANOVAs yielded significant main effects of pattern for all three parameters. ( $\alpha$ : [ $F_{(2,32)}=8.89$ ,  $p=0.001$ ,  $\eta^2=0.18$ ],  $\gamma$ : [ $F_{(2,32)}=70.85$ ,  $p<0.001$ ,  $\eta^2=0.50$ ],  $m$ : [ $F_{(1.47,23.15)}=56.73$ ,  $p<0.001$ ,  $\eta^2=0.65$ ]). Pairwise comparisons for  $\alpha$  revealed that estimates for pattern 3 differed from the estimates of pattern 1 ( $p<0.005$ ). For  $\gamma$ , pairwise comparisons showed that estimates were lower for pattern 1 compared to pattern 2 and 3, and for pattern 2 compared to pattern 3 (all  $p<0.001$ ). Pairwise comparisons for  $m$  revealed that estimates for pattern 3 were higher compared

<sup>1</sup>Due to parameter interdependence, it was necessary to restrict the parameter space of  $\alpha$  between  $-0.8$  and  $-0.1$  in order to obtain reliable and unbiased estimates. This range was based on the results of Monte-Carlo simulations.

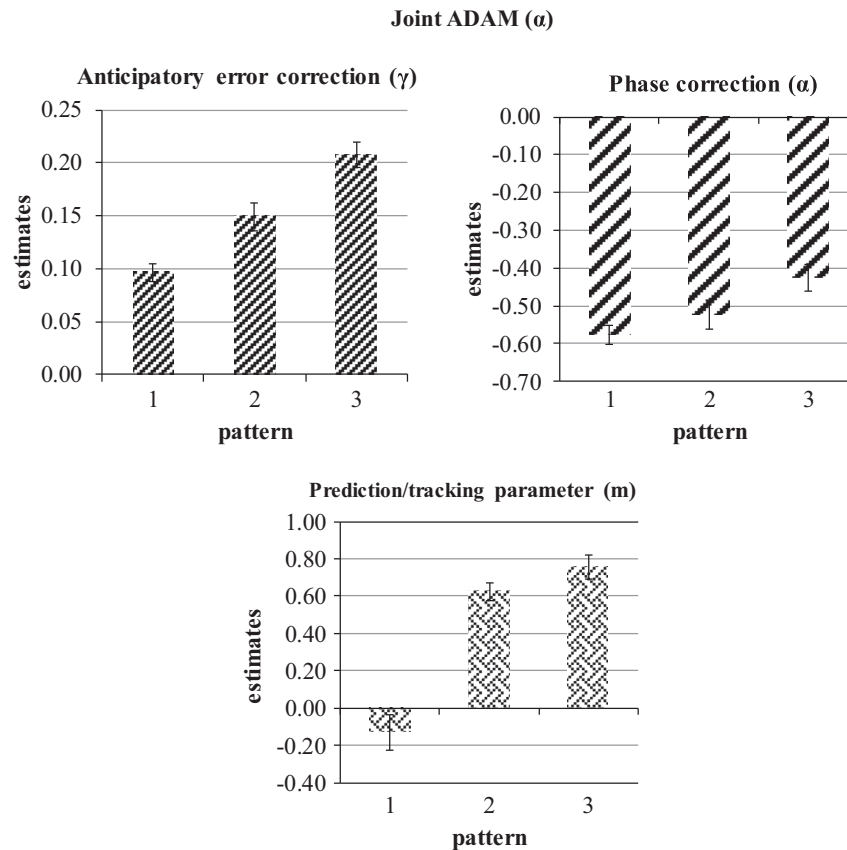


**Fig. 8 – Parameter estimates based on the ‘Joint ADAM ( $\alpha$ )’ model.  $\gamma$  reflects an anticipatory error correction process in the joint module,  $\alpha$  reflects the phase correction parameter of the adaptation module, while  $m$  indicates the prediction/tracking parameter of the anticipation module. Error bars represent standard error of parameter estimates across participants.**

to the estimates of pattern 1 ( $p < 0.001$ ). These results indicate that, compared to pattern 1 (where the rate of tempo change was lowest),  $\alpha$  estimates were less negative for patterns 3 (less phase correction in opposite direction in the adaptation module). Estimates of  $\gamma$  increased across patterns, indicating that the proportion of each anticipated asynchrony that was corrected by anticipatory error correction was smaller. Furthermore, estimates of  $m$  were low (indicating tracking) for pattern 1, while for pattern 2 and 3, where tempo changes are more frequent, estimates of  $m$  were high (indicating prediction) (Fig. 8). Note that this is more consistent with the behavioral results for PT-ratios than PT-indices.

The repeated measures ANOVA on the three parameter estimates for the ‘Joint ADAM ( $\beta$ )’ model<sup>2</sup> yielded significant main effects of pattern for  $\gamma$  estimates [ $F_{(2,32)} = 49.68$ ,  $p < 0.001$ ,  $\eta^2 = 0.41$ ] and estimates of  $m$  [ $F_{(2,32)} = 65.79$ ,  $p < 0.001$ ,  $\eta^2 = 0.65$ ]. Pairwise comparisons revealed that both the  $\gamma$  and  $m$  estimates for pattern 1 differed from estimates for pattern 2 and 3, and that estimates for pattern 2 differed from the estimates of pattern 3 (all  $p < 0.05$ ). These results suggest that the  $\gamma$  estimates increased (less anticipatory error correction [ $1 - \gamma$ ] in the

joint model) and the estimate for  $m$  increased (more tempo-change prediction) across patterns. Estimates of  $\beta$  did not show significant difference across the three patterns (Fig. 9).

### 2.3.2. Fit of the models to data

The fit of the models to the behavioral data was assessed by a log likelihood estimation procedure. Values that are less negative (i.e., smaller in absolute magnitude) indicate better fit (Fig. 10). Likelihood estimates were entered into a repeated-measures ANOVA with pattern (1–2–3) and model (‘Adaptation Model’, ‘Hybrid ADAM’, ‘Joint ADAM ( $\alpha$ )’, and ‘Joint ADAM ( $\beta$ )’) as within subject variables.

This ANOVA revealed significant main effects of model [ $F_{(1.01,16.09)} = 211.65$ ,  $p < 0.001$ ,  $\eta^2 = 0.85$ ] and pattern [ $F_{(2,32)} = 22.35$ ,  $p < 0.001$ ,  $\eta^2 = 0.15$ ], as well as a significant interaction between both variables [ $F_{(1.88,30.05)} = 13.73$ ,  $p < 0.001$ ,  $\eta^2 = 0.20$ ]. The larger, more negative log likelihood estimates observed for adaptation model indicated that its fit was poor compared to the other models, especially for pattern 2 and 3 (Fig. 10). The fit of the three models that included adaptation and anticipation mechanisms was further investigated with a separate repeated-measures ANOVA for each pattern, with model (‘Hybrid ADAM’, ‘Joint ADAM ( $\alpha$ )’, and ‘Joint ADAM ( $\beta$ )’) as the only within subject variable. For pattern 1, no significant difference between the three models was found [ $F_{(1.44,23.14)} = 2.29$ ,  $p > 0.05$ ,  $\eta^2 = 0.002$ ] (Fig. 10B). For pattern 2 and 3, significant effects of model were found

<sup>2</sup>Due to parameter interdependence, it was necessary to restrict the parameter space of  $\alpha$  between 0 and 1 (based on the results of the simulations) in order to obtain reliable and unbiased estimates. Furthermore, the parameter space for  $m$  was restricted between 0 and 1, which covers complete tracking to complete prediction.

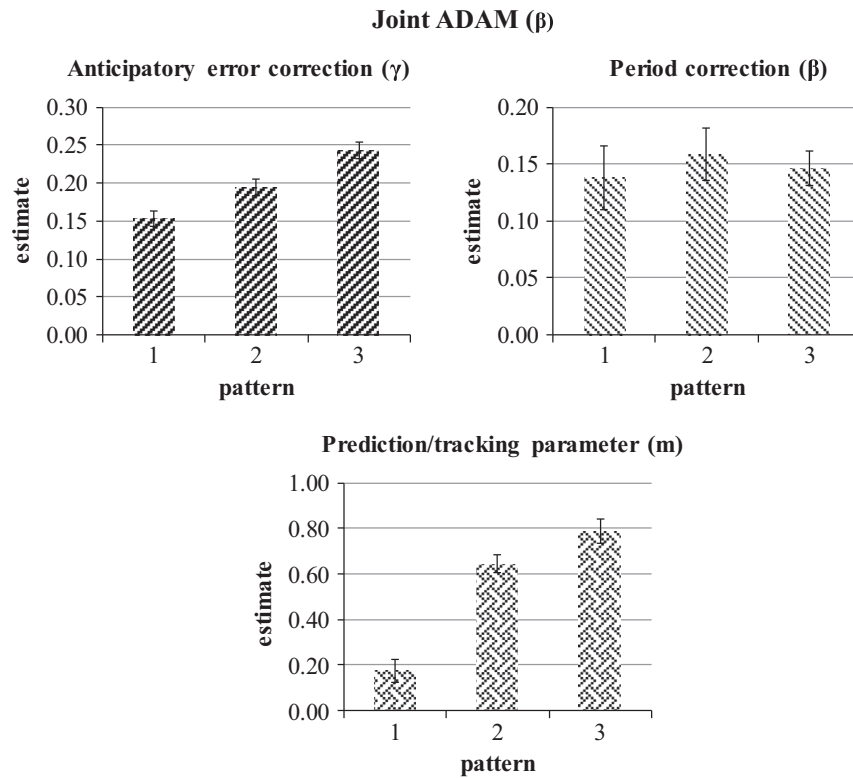


**Fig. 9** – Parameter estimates based on the ‘Joint ADAM ( $\beta$ )’ model.  $\gamma$  reflects an anticipatory error correction process in the joint module,  $\beta$  reflects the period correction parameter of the adaptation module, while  $m$  indicates the prediction/tracking parameter of the anticipation module. Error bars represent standard error of parameter estimates across participants.

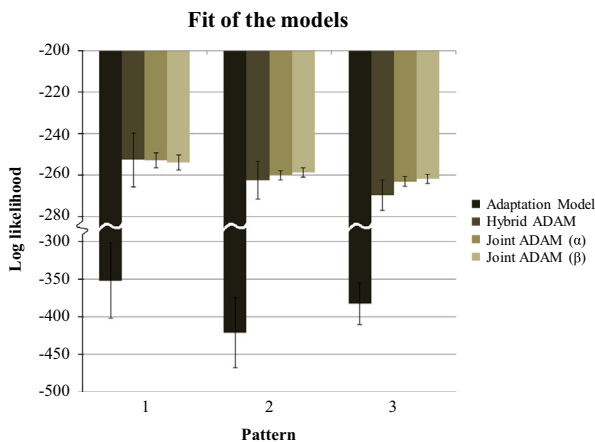


**Fig. 10** – Log likelihood estimates for the four models for each pattern. Error bars represent standard error across participants. Please note the change of the y-scale.

[pattern 2:  $F_{(1,18,18.80)}=27.49$ ,  $p<0.001$ ,  $\eta^2=0.03$ ; pattern 3:  $F_{(1,26,20.16)}=87.38$ ,  $p<0.001$ ,  $\eta^2=0.14$ ]. Pairwise comparisons for both patterns revealed that the ‘Joint ADAM ( $\beta$ )’ model had a better fit compared to the ‘Hybrid ADAM’ and ‘Joint ADAM ( $\alpha$ )’ models (all  $p<0.001$ ). Furthermore the ‘Joint ADAM ( $\alpha$ )’ model was found to have a better fit compared to the ‘Hybrid ADAM’ model (all  $p<0.001$ ). These results indicate that for pattern 2 and 3, in which the rates of tempo change are relatively high, the models in which adaptation and anticipation mechanisms are linked via a joint module, which was based on the notion of joint internal models, fit

the behavioral data better than the ‘Hybrid ADAM’ model. Overall, the ‘Joint ADAM ( $\beta$ )’ model gives the best fit to the behavioral data (Fig. 10), suggesting that participants were engaging in a mixture of period correction and anticipatory error correction.

### 3. Discussion

The aim of the current study was to investigate the contribution of temporal adaptation and anticipation mechanisms to sensorimotor synchronization with tempo changing sequences. To this end, we conducted a behavioral finger tapping experiment and ran computer simulations based on different versions of ADAM, a model of error correction (adaptation) and predictive processes (anticipation) developed by van der Steen and Keller (2013). The performance of human participants and the models was assessed with three stimulus sequences containing continuous tempo changes that were representative of expressively timed music. The sequences differed in the rate of tempo change and the number of turning points (tempo reversals). Behavioral results indicated that participants were generally capable of synchronizing with the three sequences with high levels of accuracy and precision, although SMS accuracy and precision were lowest for the pattern (3) that contained the most turning points and the largest changes in duration from interval to interval.

To shed light on the relationship between the functional roles of adaptation and anticipation mechanisms in

producing the observed behavior, simulations and model fits to the behavioral data were compared for four versions of ADAM. The simulations and model-based parameter estimates revealed that adaptation mechanisms alone (as implemented by ADAM's Adaptation module) could not fully explain the observed precision of sensorimotor synchronization. Including anticipation (in the Hybrid model, with ADAM's Adaptation and Anticipation modules active) increased the precision of simulated SMS and improved the fit of model to behavioral data. Linking adaptation and anticipation mechanisms via a joint module based on the notion of internal models led to further improvements in simulated SMS precision and model fits when the rate of tempo change was high.

These findings provide support for the hypothesis that combined adaptation and anticipation processes are required to account for human SMS behavior with tempo-changing sequences. Furthermore, the results suggest that the notion of 'anticipation' can be extended to the prediction of joint action effects through the operation of joint internal models that allow discrepancies between the outcomes of adaptive and anticipatory processes to be corrected in advance of action execution. This conceptualization of joint internal models is broadly consistent with recent developments in fields concerned with the sensorimotor and cognitive mechanisms that support social interaction in music, language, and joint action more generally (e.g., Keller et al., 2014, *in press*; Pickering and Garrod, 2013, 2014; Sebanz and Knoblich, 2009). The utility ADAM may therefore extend to multiple behavioral domains characterized by the need for interpersonal entrainment (see Phillips-Silver and Keller, 2012).

The use of pacing sequences that varied in the rate of tempo change and the number of tempo reversals yielded some findings that were not expected on the basis of previous research. First, adaptation mechanisms controlling temporal error correction did not operate entirely as expected. Contrary to our hypothesis that phase correction estimates would remain constant and that period correction would increase with the step size of the continuous tempo changes, we found that the implementation phase correction increased while period correction estimates decreased as the rate of the tempo change increased. This could indicate a stepwise or intermittent adaptation to tempo changes (Michon, 1967; Madison and Merker, 2005). Since the difference between sequential IOIs is small in continuous tempo change, it might take several tones before the perceptual threshold for tempo change is passed and period correction can be applied. Between the period adjustments, phase correction could be applied to maintain synchronization (Repp, 2005). This implies a large contribution of phase correction and a small but crucial role of stepwise or intermittent period correction when maintaining synchronization with continuous tempo changing stimulus sequences.

Consistent with the use of high amount of phase correction, employing only the 'Adaptation model' (as is the case in existing linear models of SMS; Schulze et al., 2005; Repp and Keller, 2008) yielded phase correction estimates larger than 1. These estimates suggest over-correction in the sense that participants adjusted the timing of their taps by a larger

amount than would be necessary to compensate for the full asynchrony. If no period correction is applied under such circumstances, then the timekeeper controlling tap timing does not adapt to a stimulus sequence that speeds up or slows down and the size of the tempo change is reflected in the asynchrony (Repp, 2005). Phase correction that leads to over-correction can be beneficial when dealing with continuous tempo changes as it automatically corrects the asynchrony, in which the tempo change is also reflected as the timekeeper is not updated. Period correction is effortful (Repp and Keller, 2004) and, due to the longer-lasting effects of adjusting the timekeeper period, costly to implement, as an incorrect period setting would cause continuous impairment to SMS. Stepwise or intermittent period correction in combination with a large contribution of phase correction might therefore be an economical approach especially when dealing with frequent tempo changes.

The importance of anticipatory processes involving tempo-change prediction was highlighted in the behavioral data, simulation results, and model parameter estimates. As hypothesized, the behavioral data (PT-ratios based on lag-0 and lag-1 cross-correlations between ITIs and IOIs and PT-indices based on autoregressive modeling of prewhitened ITI and IOI series) suggested participants were found to implement tempo-change predictions for all three patterns. However, PT-ratios increased with increasing degree of tempo change between successive intervals (from pattern 1 to 3), indicating that there was a tendency to engage in more predictive behavior when differences in tempo from interval to interval were larger. This is in line with previous research showing that humans predict tempo changes to the extent that the changes are detectable (e.g., Rankin et al., 2009; Pecenka and Keller, 2011). The high correlations between the PT-ratios and the PT-indices suggest that both measures generally reflect the tendency to predict tempo changes in a similar way. However, the PT-ratios turned out to behave more consistently than PT-indices with the  $m$  parameter controlling prediction and/or tracking behavior in ADAM's anticipation module. This might be seen as a reason to favor the PT-ratios over PT-indices, or at least to consider both measures, when describing anticipatory behavior in human SMS across different types of tempo changing sequences.

Simulations, parameter estimates, and model fitting procedures clearly favored the inclusion of ADAM's anticipation module to account for human SMS with tempo changes. Specifically, in terms of fit, the adaptation model turned out to be inferior to the models that combined adaptation and anticipation for the three rates of tempo change that we investigated. In fact, the 'Joint ADAM ( $\beta$ ) model' – given that it accounted most closely for the highest rate of tempo change that we examined (pattern 3) – was found to have the best fit of the models that were tested in the current study. A recent study of SMS in patients with lesions to the basal ganglia and cerebellum found converging evidence for the validity of joint models linking adaptation and tempo-change prediction during synchronization with tempo changing sequences (van der Steen et al., *in press*). It should, however, be noted that, due to parameter interdependence for both joint models, the parameter space needed to be restricted in order to be able to obtain reliable estimates (especially for pattern 1) in

the current study. For the 'Joint ADAM ( $\beta$ )' model, the  $m$  estimate for pattern 1 was set to zero (complete tracking) in 63% of the trials, indicating that the  $m$  estimate reached the restriction. For pattern 2 and 3, this happened in only 3% and 1.5% of the trials, respectively. This suggests that the joint model had some difficulties when dealing with relatively small tempo changes (for pattern 1, where the difference between two successive IOIs was only in the range 1–14 ms) and might indicate that prediction does not play a big role under such circumstances. Furthermore, for both 'Joint ADAM ( $\alpha\beta$ )' and the 'Hybrid ADAM' model,  $m$  estimates close to zero were found for pattern 1. This implied tracking behavior instead of the prediction of the tempo changes suggested by the PT-ratios computed from the behavioral data. It might be the case that adaptation and anticipation mechanisms are linked differently (e.g., non-linearly), and that adaptation plays a greater role, when dealing with small tempo changes than when tempo changes are larger and easier to detect (van der Steen et al., in press). Previous studies have shown that tempo changes are not fully predicted if these changes are small enough to be subliminal (Thaut et al., 1998b; Madison and Merker 2005). Nevertheless, synchronization can be established in these situations solely through the operation of adaptation mechanisms.

While ADAM performed well in terms of furthering our understanding of the role of temporal adaptation and anticipation in SMS with tempo-changing sequences, there are several issues that should be addressed in future research. One of these relates to using either phase or period correction in the 'Joint ADAM' models and setting the other parameter to zero, instead of combining both adaptation mechanisms in one model. In this study, we decided to limit the number of free parameters in each model. If many parameters are allowed to vary, it becomes harder to determine the estimates and to interpret the results. Furthermore, in order to compare the fit of the models using the log likelihood criterion the number of parameters needs to be equal. Note, however, that it is possible to use the closely related BIC or AICc criteria (see Brockwell and Davis, 2009) to compare between models with different number of parameters. When phase and period correction are combined in a 'Joint ADAM' model, it could be that phase correction becomes redundant. On the other hand, it could be that phase and period correction – within limits – reinforce each other as seemed to be the case in the 'Adaptation Model'.

Furthermore, the treatment of noise terms in the model should be addressed. Adding timekeeper and motor noise to the simulations influences the variability of the simulated asynchrony and the fit of the models to the data. The current simulations included motor and timekeeper noise, for which values were drawn from the same distributions for all four models. There are, nevertheless, some noise-related issues that our simulations did not address. First, we did not take into account that timekeeper variance increases with interval length (Wing, 1980). Such dependence could have led to the scaling of SMS precision as intervals became progressively longer or shorter in each pattern. Second, we did not include perceptual noise, which affects the perceived time of occurrence of the stimulus, the participants' own taps, and therefore the perceived asynchrony (Repp and Keller, 2004).

Variability in perceived timing also increases with interval length (Frigberg and Sundberg, 1995; Repp, 2006). Notwithstanding these issues, it was still possible to determine model fits with respect to the behavioral data in the current study since we applied noise in a similar way for all four models.

Another issue in need of clarification concerns evidence found for 'negative' error correction. The negative  $\alpha$  estimates for the 'Hybrid ADAM' and especially the 'Joint ADAM ( $\alpha$ )' model were unexpected and remain puzzling. For the 'Joint ADAM ( $\alpha$ )' model, estimates had to be restricted to a negative range in order to obtain reliable estimates with the bGLS-method. We used Monte Carlo simulations to determine the range of values to which the parameter space was restricted. According to Vorberg and Schulze (2002), phase correction in a range between 0 and 2 facilitates stable SMS (i.e., minimal variability of asynchronies). Negative phase correction suggests a local correction in a direction opposite to the asynchrony, which normally does not contribute to successful SMS. However, anticipation mechanisms tend to lead to predictions that over- and undershoot at turning points. During synchronization with tempo changing sequences that contain tempo reversals, implementing corrections in the opposite direction could thus have a positive effect on SMS because such corrections counteract this imprecision in predictions. The slightly negative  $\alpha$  estimates for the 'Hybrid ADAM' model, in conjunction with  $m$  estimates that indicate prediction, might thus in fact have been beneficial to stable SMS. Further behavioral and modeling work is needed to test this hypothesis.

Finally, there is scope for further development in relation to ADAM's anticipation module. One issue concerns the relationship between the prediction/tracking parameter  $m$  implemented in ADAM and the concept of 'anticipatory period correction' described by Repp (2006). According to Repp (2006), expectations and active prediction of learned timing are employed to adjust the period of the internal timekeeper that controls movement timing during SMS. On this view, anticipatory period correction improves with exposure to a specific pattern due to learning and the formation of memory representations, resulting in smaller asynchronies and thus better synchronization. In ADAM, the parameter  $m$  regulates the balance between tempo-change prediction (based on linear extrapolation of pacing sequence IOIs) and tracking (copying the previous pacing IOI). Unlike anticipatory period correction, however, the parameter  $m$  is not used explicitly to set the timekeeper. Future work could explore whether there is scope for such a process, as it would allow the role of memory for specific patterns of tempo change to be accommodated in ADAM.

Another issue concerning ADAM's anticipation module is the extent of temporal extrapolation involved in tempo-change prediction. The number of intervals used in the linear extrapolation process implemented by ADAM is controlled by varying the parameter  $k$  in the anticipation module (van der Steen and Keller, 2013). In the current simulations,  $k$  was set to 2, indicating that the predictions were an extrapolation based on the previous two intervals. Although using more intervals would make predictions more robust against outliers, this also means it takes longer before a change in direction of the tempo change (i.e., turning point) is detected

and processed. Since the current patterns followed a clear sigmoidal function, basing predictions on just two intervals led to the most accurate results. If less predictable or more variable human sequences were to be used, then a higher value of  $k$  might be necessary for optimal anticipation.

Related to the previous point is the current usage of a first-order linear extrapolation process. This process detects and works with the direction and magnitude of a tempo change in such a way that an accelerating sequence (with intervals that decrease in duration) will result in a prediction that the next event will occur after an even shorter interval, and vice versa for tempo deceleration. It has been demonstrated that attending to and predicting such tempo changes is beneficial during SMS (Pecenka and Keller, 2011; Pecenka et al., 2013). However, it is not being claimed that human tempo-change prediction is limited to first-order linear extrapolation. More complex prediction processes—such as higher-order fitting and long-range correlations, or, when dealing with music, processes that take into account hierarchically nested timescales associated with metrical structure—might be applied during synchronization with sequences characterized by richer temporal and sequential structure (e.g., Drake et al., 2000; Rankin et al., 2009).

Overall, we conclude that temporal adaptation and anticipation mechanisms both make vital contributions to successful SMS behavior, specifically for SMS with tempo changes such as those found in expressively performed music. Exactly how adaptation and anticipation mechanisms interact under such conditions remains an open question. Nevertheless, our results are consistent with the proposal that joint internal models that evaluate the degree of discrepancy between adaptation and anticipation, and allow any potential error to be compensated for before it occurs, play a role in linking these mechanisms. By allowing such processes to be interrogated, ADAM has proven to be a useful framework for investigating the role of adaptation and anticipation during SMS, and how these mechanisms might interact. It would be fruitful in future research with ADAM to explore different types of linkage between the adaptation and anticipation modules (e.g., by including phase and period correction in a joint model), to address the role of the different noise components (e.g., perceptual noise), and to include other (visual) synchronization cues associated with body movements and hierarchical temporal structures, such as those occurring in music performance.

## 4. Experimental procedure

### 4.1. Experiment

#### 4.1.1. Participants

Twenty amateur musicians (11 female/9 male, age:  $25.83 \pm 4.25$  years, musical experience:  $18.15 \pm 3.98$  years) participated in this study. Participants played a variety of instruments, often multiple, including piano, guitar, violin, flute, accordion, drums, trombone, and horn. None of the participants reported any neurological or psychiatric disorders. Participants received written descriptions of all procedures and signed an informed consent form before the experiment started. Data from three participants were excluded from the final sample ( $N=17$ ) due to

technical problems ( $n=2$ ) and failure to reach criterion performance ( $n=1$ ).

#### 4.1.2. Materials

Three different patterns served as stimulus sequences (Fig. 2). All patterns started with a section in which the tempo was stable, consisting of 16 tones (woodblock, 25 ms duration) with IOIs of 600 ms. This section was included in order to allow synchrony to be established between the stimulus sequence and the participants' taps. The IOIs of the following 48 sequence tones gradually changed between 600 ms and 400 ms. The tempo changes were designed to resemble musical *accelerando* and *ritardando* and followed a sigmoidal function (cf. Schulze et al., 2005)<sup>3</sup>. The three patterns differed in the number of steps ( $N_{steps}$ ) required to cover the 200 ms change in IOI. Since the tempo-changing section of all patterns contained the same number of beats (48), the number of steps used to cover the change meant that the three patterns differed in the number of cycles that contained this tempo change. An *accelerando* phase followed by a successive *ritardando* phase constituted one cycle of tempo change from an IOI of 400 ms to 600 ms and back to 400 ms (Fig. 2).

In Pattern 1, the *accelerando* and *ritardando* phases of the tempo change each spanned 24 steps. This led to one cycle per trial that changed tempo smoothly and slowly, with the difference between successive IOIs being small (range: 1–14 ms). Pattern 2 had 12 steps for each *accelerando* and *ritardando* phase, and hence contained two cycles (each of 24 steps) of speeding up and slowing down (the difference between successive IOIs ranged between 4 and 28 ms). In Pattern 3, there were 8 steps for each *accelerando* and *ritardando* phase, leading to three cycles (consisting of 16 steps each) of rapid and large tempo changes (successive IOI differences ranged from 10 to 44 ms) (Fig. 2).

#### 4.1.3. Procedure

The current dataset was obtained as part of a large-scale experiment examining participants' abilities to learn to tap the three different patterns of tempo change. In the experiment, participants tapped the three patterns under three conditions that were presented in a fixed order. First, in a 'Melody' condition, participants tapped along with the melody line of a Bach chorale presented in a piano timbre<sup>4</sup>. The tempo of melody line was set to follow the tempo-changing pattern as described above (Fig. 2). Second, in a 'Pacing signal' condition, participants synchronized their taps with the

<sup>3</sup>The sigmoidal function was defined by:

$$IOI_i = tempo_{goal} + (tempo_{start} - tempo_{goal}) \times frac \quad (1')$$

$$frac = \frac{1}{2} \left[ 1 + \cos \frac{i-1}{N_{steps}-1} \pi \right] \quad (2')$$

For the *accelerando* part of each cycle  $tempo_{start}$  was set to 600 and  $tempo_{goal}$  was 400. For the *ritardando* part of each cycle  $tempo_{start}$  was set to 400 and  $tempo_{goal}$  was 600.  $N_{steps}$  is the number of steps available to cover to 200 ms change in IOI. The index of the IOI is represented by  $i$ .

<sup>4</sup>Half, dotted, and 8th notes in the chorale were transformed, using Finale<sup>®</sup> software, into quarter notes to end up with 64 events of equal length.

tempo-changing stimulus signals that used a woodblock sound for each note of the chorale (instead of the piano timbre). Third, in a 'Free' condition, participants tapped the tempo-changing pattern by themselves in a self-paced manner without an auditory synchronization aid. All conditions started with 4 initiation tones indicating the initial tempo (600 ms IOI). During all conditions the musical notation of the chorale including the tempo changes was displayed on a computer monitor in front of the participant. The three patterns were presented in an order randomized that was across participants. Each condition (Melody, Pacing signal, Free) for each pattern started with a practice trial, followed by 15 experimental trials, each lasting 35 s.

Participants were seated in a quiet laboratory room and were instructed to tap the tempo-changing sequences as accurately and precisely as possible. Participants' taps did not trigger sounds. The experiment was run in Presentation (Neurobehavioral Systems, <http://www.neurobs.com>) on a Windows computer. Participants' timing was registered using a custom built tapping device that was connected to the computer via a serial connection. Auditory information was presented over headphones. Participants started each trial by pressing a key on a keyboard and could therefore pace their progression through the experiment. Short breaks between patterns were allowed. In total the experiment took 1.5–2 h. The current article is based on the synchronized tapping data obtained in the 'Pacing signal' condition.

#### 4.1.4. Data-analyses

The onset times of taps were aligned offline to the closest tones of the target sequence within  $\pm 200$  ms asynchrony window<sup>5</sup>. 2.6% of the recorded taps fell outside this window and were excluded from the analyses. Data analyses focused on the tempo-changing phase of the trials (Fig. 2), the stable phase was used to establish synchrony between the stimulus sequence and the participants' taps [mean/SD of signed asynchrony (mean  $\pm$  SD):  $-18.4 \pm 16.1/19.1 \pm 3.5$  ms (pattern 1),  $-17.9 \pm 16.1/19.3 \pm 3.8$  ms (pattern 2);  $-24.3 \pm 16.1/19.0 \pm 3.3$  ms (pattern 3)]. The mean signed asynchrony was calculated as an inverse measure of SMS accuracy, while the standard deviation of the signed asynchronies was used as an inverse measure of SMS precision. SMS accuracy and SMS precision measures were calculated for each trial and then averaged across repetitions of each pattern for each participant.

Before measures related to the hypothesized underlying adaptation and anticipation mechanisms were calculated, linear interpolation was used to fill missing asynchronies, unusually large ITIs, and missing ITIs resulting from skipped taps. This affected less than 1% of data. To investigate adaptation while synchronizing with tempo-changing sequences, the amount of phase and period correction implemented by the participant was estimated by means of the bGLS method (cf., [Jacoby and Repp, 2012](#) see also [Jacoby et al., in press](#) for further analysis of the method) based on the adaptation model ([Schulze et al., 2005](#); [Repp and Keller, 2008](#)). In this model, both correction mechanisms depend on the preceding asynchrony.

<sup>5</sup>There was a transmission delay of 10 ms between the tapping device and the registration software, which was subtracted from the recorded tap times before data analysis.

The bGLS method used the interpolated inter-tap intervals and corresponding asynchronies as input (A detailed description of the method can be found in [Appendix A](#)).

Anticipation during synchronization with tempo-changing sequences was quantified using two methods. The first was based on the lag-1 and lag-0 cross-correlations between the inter-stimulus and inter-tap intervals and the prediction/tracking ratio. The lag-0 cross-correlation between the IOIs and ITIs is high to the extent that participants anticipate the tempo changes, while the lag-1 cross-correlation is high to the extent that participants copy, or 'track', the tempo changes. This relationship reflected in the PT-ratio (lag-0/lag-1 cross-correlation) used by [Pecenka and Keller \(2009, 2011\)](#). A ratio bigger than 1 reflects the participant's tendency to predict the tempo change, while ratio smaller than 1 indicates that the participant tend to copy (track) the tempo changes. It has been shown that autocorrelations of time series might influence cross-correlation estimates ([Dean and Bailes, 2010](#)). Therefore, we also investigated the anticipation mechanisms by means of alternative PT-indices ([Mills et al., in press](#)). PT-indices are based on the difference between the coefficients of two autoregressive components of the autoregressive model ([Dean and Bailes, 2010](#); [Launay et al., 2013](#)). Prior to applying the autoregressive model, IOI and ITI time series were pre-whitened. Pre-whitening consists of identifying the autoregressive lag structure of one series, and calculating residuals after the influence of the autoregressive structure has been modeled ([Dean and Bailes, 2010](#)). The autoregressive model was then used to calculate the coefficients representing the strength of the relationship between IOIs and ITIs using pre-whitened IOI series at lag-0 and lag-1 as predictors for the pre-whitened ITI series. In a final step, the lag-1 coefficient was subtracted from the lag-0 coefficient, resulting in an index with values greater than 0 reflecting anticipation of the tempo changes in the patterns and values smaller than 0 reflecting tracking behavior ([Mills et al., in press](#)).

The data were processed with MATLAB (The Mathworks Inc., MA, USA R 2011a). Statistical analyses were performed with SPSS (IBM SPSS Statistics 21). In addition to descriptive statistics, repeated measures ANOVAs were conducted to test for effects of the factors (e.g., pattern). Generalized eta-squared values were computed as a measure of effect size to aid in interpreting the significant effects from the analyses of variance. If the assumption of sphericity was violated, the Greenhouse–Geisser correction was applied. The Bonferroni method was used to correct for multiple pairwise comparisons. Adjusted *p*-values are reported.

## 4.2. Simulations

To investigate the effect of adaptation and anticipation mechanisms on SMS precision, we ran simulations with ADAM in which parameter settings were systematically varied. We focused on SMS precision because in a previous study adaptation mechanisms were found to contribute more to SMS accuracy, while both adaptation and anticipation mechanisms predicted SMS precision ([Mills et al., in press](#)). Possible links between the adaptation and anticipation

mechanisms were explored by creating four different versions of ADAM.

Input values for the simulations were the onset times that correspond to three different tempo-changing patterns. The output for all versions consisted of the simulated tap times. For each pattern and parameter setting combination, 1000 trials are simulated in MATLAB (The Mathworks Inc, MA, USA R 2011a). Timekeeper noise was sampled from a normal distribution, while motor noise was drawn from a gamma distribution (Repp and Keller, 2008). The standard deviation of asynchronies was taken as a measure of a SMS precision in simulated data. Asynchronies were computed as the difference between the onset times of simulated tones in the tempo-changing pattern and the simulated tap times, and were, by convention, negative if the simulated tap preceded the tone onset time.

#### 4.2.1. Background

ADAM comprises an adaptation and anticipation module (van der Steen and Keller, 2013). The adaptation module of ADAM implements phase and period correction following the equations<sup>6</sup>:

$$t_{n+1} = t_n + T_n - (\alpha + \beta) \times asyn_n + TK_n + M_n - M_{n-1} \quad (1)$$

$$T_{n+1} = T_n - \beta \times asyn_n \quad (2)$$

The most recent asynchrony ( $asyn_n$ ) is multiplied by the sum of the phase ( $\alpha$ ) and period ( $\beta$ ) correction parameters and the result is added to the current timekeeper period ( $T_n$ ) (Eq. (1)). The timing of the next tap ( $t_{n+1}$ ) by ADAM is then determined by adding this to the timing of the most recent event ( $t_n$ ). Timekeeper (TK) and motor noise (M) is added so that ADAM produces human-like asynchronies (Repp and Keller, 2008). The current timekeeper period is affected by the period correction parameter ( $\beta$ ) (Eq. (2)). The next timekeeper period ( $T_{n+1}$ ) is given by the last asynchrony ( $asyn_n$ ) multiplied by the period correction parameter ( $\beta$ ) added to the current timekeeper ( $T_n$ ).

The anticipation module of ADAM bases the timing of the next tap on a temporal extrapolation process that generates a prediction about the timing of the next tone based on the most recent series of IOIs that ADAM receives as input. The predicted time of the next tone ( $tone_{n+1}$ ) is based on Eq. (3)<sup>7</sup>, where Eq. (4)<sup>8</sup> is used to determine the predicted interval

( $Int_{n+1}$ ):

$$tone_{n+1} = tone_n + Int_{n+1} \quad (3)$$

$$Int_{n+1} = a + b \times (n + 1) \quad (4)$$

$$t_{n+1} = tone_{n+1} - \alpha \times asyn_n + TK_n + M_n - M_{n-1} \quad (5)$$

In Eq. (4),  $a$  represents the intercept and  $b$  stands for the slope of the best fitting line. Both parameters  $a$  and  $b$  depend on the number in intervals ( $k$ ) used to determine the best-fitting straight line. The onset time of the next tap is set to match the predicted tone onset time. Like in the adaptation module the tap is subject to noise (Eq. (5)).

The adaptation and anticipation module can be linked in different manners. In the current study we investigate a hybrid link in which error correction is applied on the basis of predicted tempo changes and a link based on the notion of joint internal models (see below).

#### 4.2.2. Models

In the ‘Adaptation Model’, only the adaptation module of ADAM (which implements phase and period correction) is active (Eqs. (1) and (2)). The adaptation module determines the proportion of each asynchrony that will be compensated for in the planning of the next movement.

In the ‘Hybrid ADAM’ model, the adaptation and anticipation modules are both active. As in the ‘Adaptation Model’, the adaptation module in ‘Hybrid ADAM’ model determines the proportion of each asynchrony that will be compensated for. The anticipation module predicts the timing of the upcoming pacing tone. In the ‘Hybrid ADAM’ model, this prediction is used to set a provisional time for the next tap (Fig. 11). The anticipation module takes into account that humans can engage in tempo-change prediction and tracking behavior at the same time by predicting the timing of the next event in a pacing sequence based the weighted sum of two processes ( $m$ ) (Eq. (10)). Thus, for tempo-change prediction the interval ( $Int_{n+1}$ ) between the current and next tone ( $tone'_{n+1}$ ) (Eq. (6)) is derived through a temporal extrapolation process (as described above) based on two most recent IOIs ( $k=2$ ) (Eq. (7)). By means of predictive behavior, the interval ( $PRED_{n+1}$ ) needed for a tap to be aligned with the simulated next tone ( $tone_{n+1}$ ) is determined (Eq. (8)). Tracking behavior leads to in interval ( $TRACK_{n+1}$ ) of the size of the previous IOI (Eq. (9)). Because predictions are not necessarily correct and the system is subjected to noise, the output of the adaptation module is used to apply a local correction to simulate the process of counteracting unintentional variability. Therefore, the timing of the next tap ( $t_{n+1}$ ), determined by the anticipation module, is also subjected to phase correction ( $\alpha$ ) (Eq. (10)). The application of error correction in the ‘Adaptation Model’

(footnote continued)

The smallest sum of squared errors is obtained if

$$b = \frac{k \times \sum_{i=1}^k x_i \times Int - \sum_{i=1}^k x_i \times \sum_{i=1}^k Int}{k \times \sum_{i=1}^k x_i^2 - \sum_{i=1}^k x_i \times \sum_{i=1}^k x_i}$$

and

$$a = \frac{1}{k} \times \sum_{i=1}^k Int_i - \frac{1}{k} \times b \times \sum_{i=1}^k x_i.$$

<sup>6</sup>The difference in sign compared to the equations in van der Steen and Keller (2013) is because in this case ADAM takes the role of participant while in the other paper ADAM presents the pacing tones.

<sup>7</sup>The equations are slightly modified compared to the equations in van der Steen and Keller (2013) since in the current paper ADAM takes the role of participant and thus produces taps while in the previous paper ADAM controlled the pacing tones.

<sup>8</sup>Following the method of least squares, the line of the form  $Int = a + b \times x$  has the smallest sum of squared errors if

$$a \times k + b \times \sum_{i=1}^k x_{n-k+i} = \sum_{i=1}^k Int_{n-k+i}$$

and

$$a \times \sum_{i=1}^k x_{n-k+i} + b \times \sum_{i=1}^k (x_{n-k+i})^2 = \sum_{i=1}^k (x_{n-k+i} \times Int_{n-k+i}).$$

<b>Hybrid ADAM</b>	
Interval prediction:	
$tone'_{n+1} = tone_n + Int_{n+1}$	(6)
$Int_{n+1} = a + b * (n + 1)$	(7)
$PRED_{n+1} = tone'_{n+1} - t_n$	(8)
Interval tracking:	
$TRACK_{n+1} = tone_n - tone_{n-1}$	(9)
$t_{n+1} = t_n + (m * PRED_{n+1} + (1 - m) * TRACK_{n+1}) - \alpha * asyn_n + TK_n + M_n - M_{n-1}$	(10)
<b>Joint ADAM</b>	
<u>Adaptation module*</u> :	
$t'_{n+1} = t_n + T_n - (\alpha + \beta) * asyn_n + TK1_n$	(11)
$T_{n+1} = T_n - \beta * asyn_n$	(12)
* Joint ADAM ( $\alpha$ ), we assume $\beta = 0$	
Joint ADAM ( $\beta$ ), we assume $\alpha = 0$	
<u>Anticipation module:</u>	
$IOI\_pred_{n+1} = Int_{n+1} = a + b * (n + 1)$	(13)
$IOI\_track_{n+1} = tone_n - tone_{n-1}$	(14)
$tone'_{n+1} = tone_n + (m * IOI\_pred_{n+1} + (1 - m) * IOI\_track_{n+1}) + TK2_n$	(15)
<u>Joint module:</u>	
$asyn'_{n+1} = t'_{n+1} - tone'_{n+1}$	(16)
$t_{n+1} = t'_{n+1} - ((1 - \gamma) * asyn'_{n+1}) + M_n - M_{n-1}$	(17)

**Fig. 11** – Equations describing the ‘Hybrid ADAM’ and ‘Joint ADAM ( $\alpha/\beta$ )’ models.  $\alpha$ =phase correction,  $\beta$ =period correction,  $\gamma$ =anticipatory error correction,  $m$ =prediction/tracking parameter. See text for explanation.

and the ‘Hybrid ADAM’ model differs in the sense that, in the ‘Adaptation Model’, compensatory adjustments are made to the current timekeeper period, while in the ‘Hybrid ADAM’ model, the adjustments are made to the output of the anticipation module (i.e., the next predicted IOI).

In the ‘Joint ADAM ( $\alpha$ )’ and ‘Joint ADAM ( $\beta$ )’ models, again both the adaptation and the anticipation modules of ADAM are active and linked in a joint module (Fig. 11). In the ‘Joint ADAM ( $\alpha$ )’ model, the timing of the next tap ( $t_{n+1}$ ) is simulated by the adaptation module. The most recent asynchrony ( $asyn_n$ ) is multiplied by the phase correction parameter ( $\alpha$ ) and added to the timing of the previous tap ( $t_n$ ) and the current, unaffected, timekeeper period ( $T_n$ ) (Eq. (11)). In the ‘Joint ADAM ( $\beta$ )’ model, the timing of the next tap ( $t_{n+1}$ ) is also simulated by the adaptation module, but this time the most recent asynchrony ( $asyn_n$ ) is multiplied by the period correction parameter ( $\beta$ ) and added to the previous timekeeper ( $T_n$ ) (Eq. (12)). The timekeeper period ( $T_{n+1}$ ) is thus affected by period correction. The simulated timing of the next tap ( $t_{n+1}$ ) is therefore equal to the timing of the previous tap ( $t_n$ ) in combination with the new timekeeper period ( $T_{n+1}$ ) and the corrected asynchrony ( $asyn_n \times \beta$ ) (Eq. (11)). In both versions of the Joint model, the anticipation module predicts when the next tone ( $tone'_{n+1}$ ) will occur (Eq. (15)). This next tone is a weighted sum of predictive behavior, i.e., extrapolation based on two most recent IOIs ( $k=2$ ) (Eq. (13)), and tracking behavior, which copies the previous interval (Eq. (14)). Predictive and tracking processes are regulated by the prediction/tracking parameter ( $m$ ) (Eq. (15)). Theoretically, this parameter ranges from 0 to 1, with  $m=0$  indicating that the model relied fully on tracking, while with  $m=1$  the next tone is based purely on temporal extrapolation. The joint module simulates the asynchrony ( $asyn'_{n+1}$ ) between the planned next tap ( $tone'_{n+1}$ ) and the predicted next tone ( $tone'_{n+1}$ ) (Eq. (16)). This simulated asynchrony is then minimized by means of

an anticipatory error correction process ( $\gamma$ ), which influences occurrence of the next tap ( $t_{n+1}$ ) (Eq. (17)). The appropriate motor command is then selected to execute this next tap ( $t_{n+1}$ ). In both ‘Joint ADAM’ models potential errors are thus predicted and corrected before they could occur. The adaptation and anticipation modules are subjected to timekeeper noise (TK), while motor noise (M) affects the next tap in the link process in the joint module.

#### 4.3. Evaluation of the models

Parameter estimates for the different models were obtained from the behavioral data by means of the bGLS method (Repp et al., 2012; Jacoby et al., in press). The method is based on rewriting each model in a matrix notation. Based on this notation a solution to a generalized regression problem is found, with certain constraints imposed on the parameter spaces (Appendix A). Furthermore, we normalized the asynchrony time series by subtracting the mean asynchrony from each asynchrony. Due to parameter interdependence in the joint models it was necessary to restrict the parameter space in order to obtain reliable and unbiased estimates. Monte Carlo simulations were run to determine the range of values to which the parameter space was restricted. For the ‘Joint ADAM ( $\alpha$ )’ model,  $\alpha$  values were restricted to the range  $-0.8 < \alpha < -0.1$ . For the ‘Joint ADAM ( $\beta$ )’ both  $\beta$  and  $m$  were restricted ( $0 < \beta, m < 1$ , see Appendix A).

The fit of the model is determined by the log likelihood estimate. The log likelihood of the model is related to the generalized sum of squares and defined as  $LL = \log_2(p(\text{data model}))$ , where  $p$  is the probability. The log likelihood is computed assuming a multivariate normal distribution (Jacoby et al., in press). A less negative and smaller in absolute value indicated a better fit between the behavioral data and the model. When calculating the likelihood, the

same data and number of estimated parameters were included for all models. Therefore, for both joint models, the motor noise parameter was set to zero.

### Author contributions

Design research: MS, MT, PK/Perform research: MS/Data analyses: MS, NJ/Writing manuscript: MS, NJ, MT, PK.

### Conflict of interest statement

The authors declare that there is no conflict of interest.

### Acknowledgments

We thank Felix Haiduk, Kerstin Traeger, and Maria Bader for their help preparing and running the behavioral experiment. We thank Twan Dollevoet for his help with re-formulating the equations for the bGLS method and his comments on an earlier version of the manuscript. Furthermore we thank the reviewers for their thorough and constructive comments.

This work was supported by funding from the European Community’s Seventh Framework Programme under the EBRAMUS project—grant agreement no. 238157. The funders had no role in study design, data collection and analysis, decision to publish, or preparation of the manuscript.

### Appendix A. Estimating the model parameters with the bGLS method

We used the bGLS method to estimate the models’ parameters (Repp et al., 2012; Jacoby et al., in press). The method is based on re-writing the model in matrix notation. Based on this notation a generalized regression problem is solved, with certain constraints imposed on the parameter space.

In order to match the notation of (Jacoby et al., in press) we will introduce slightly different notation to that used in the main body of the article.

We denote by  $S(n)$ ,  $R(n)$  the stimulus and response onsets at time  $n$ , respectively. We denote by  $s(n)$  and  $r(n)$  the inter-stimulus and inter-response intervals, respectively. We denote by  $e(n)$  the asynchrony:  $e(n)=R(n)-S(n)$ . This leads to the following relations:

$$tone_n = S(n), \tag{A1}$$

$$IOI = s(n), \tag{A2}$$

$$t_n = R(n), \tag{A3}$$

$$ITI = r(n), \tag{A4}$$

$$asyn_n = e(n). \tag{A5}$$

We denote by  $z(n)$  the noise at time  $n$ . The assumption is that  $z$  has two components: a motor and a time keeper variance, similar to the model of Vorberg and Wing (1996).

$$z(n) = TK(n) + M(n) - M(n-1), \tag{A6}$$

where  $TK(n)$  and  $M(n)$  are the timekeeper and motor noises with variance  $\sigma_T^2$  and  $\sigma_M^2$ , respectively.

We will focus on the model where the prediction is based on the two recent intervals ( $k=2$ ). In this case it follows that the slope of the best fit equals  $s(n) - s(n-1)$ . Hence,

$$Int_{n+1} = s(n) + (s(n) - s(n-1)) = 2 \times s(n) - s(n-1) \tag{A7}$$

In what follows we rewrite Joint ADAM ( $\alpha$ ), Joint ADAM ( $\beta$ ), and Hybrid ADAM as a bGLS regression model.

### Joint ADAM ( $\alpha$ )

ADAPTATION module:

$$t_{adap_{n+1}} = t_n + T_n - (\alpha + \beta) \times asyn_n + TK1_n$$

$$T_{n+1} = T_n - \beta \times asyn_n$$

We assume  $[\beta=0]$ , thus  $T_{n+1}=T_n=T_0$

ANTICIPATION module:

$$IOI_{pred_{n+1}} = Int_{n+1} = a + b$$

$$\times n + 1IOI_{track_{n+1}} = tone_n - tone_{n-1} tone_{anti_{n+1}} = tone_n + m \times IOI_{pred_{n+1}} + 1 - m \times IOI_{track_{n+1}} + TK2_n$$

joint module:

$$asyn_{joint} = t_{adap_{n+1}} - tone_{anti_{n+1}}$$

$$t_{n+1} = t_{adap_{n+1}} - ((1 - \gamma) \times asyn_{joint}) + M_{noise}$$

Using the new notation and  $T_n=T_0$  for all  $n$ , we write:

ADAPTATION module:

$$t_{adap_{n+1}} = R(n) + T_0 - \alpha \times en + TK1(n) \tag{A8}$$

ANTICIPATION module:

$$IOI_{pred_{n+1}} = Int_{n+1} = a + b \times (n + 1) = 2s(n) - s(n-1) \tag{A9}$$

$$IOI_{track_{n+1}} = tone_n - tone_{n-1} = s(n) \tag{A10}$$

$$tone_{anti_{n+1}} = S(n) + (m \times (2s(n) - s(n-1)) + (1 - m) \times s(n)) + TK2(n) = S(n) + (m + 1)s(n) - m \times s(n-1) + TK2(n) \tag{A11}$$

joint module:

$$asyn_{joint} = t_{adap_{n+1}} - tone_{anti_{n+1}} = [R(n) + T_0 - \alpha \times e(n) + TK1(n)] - [S(n) + (m + 1)s(n) - m \times s(n-1) + TK2(n)] = (1 - \alpha)e(n) + T_0 - (m + 1)s(n) + m \times s(n-1) + TK1(n) - TK2(n) \tag{A12}$$

$$t_{n+1} = t_{adap_{n+1}} - ((1 - \gamma) \times asyn_{joint}) + M_{noise} = [R(n) + T_0 - \alpha \times e(n) + TK1(n)] + M(n) - M(n-1) - ((1 - \gamma) \times [(1 - \alpha)e(n) + T_0 - (m + 1)s(n) + m \times s(n-1) + TK1(n) - TK2(n)]) \tag{A13}$$

This can be written as:

$$r(n + 1) + (-\gamma)T_0 = (-1 + \gamma - \alpha\gamma)e(n) + [(1 - \gamma)(1 + m)]s(n) + [(-1 + \gamma)m] \times s(n-1) + [\gamma TK1(n) + (1 - \gamma) TK2(n) + M(n) - M(n-1)] = (1 - \gamma)m \times [s(n) - s(n-1)] + (1 - \gamma) [s(n) - e(n)] + (\alpha\gamma)(-e(n)) + z(n) \tag{A14}$$

where  $z(n) = [\gamma TK1(n) + (1 - \gamma)TK2(n) + m(n)] = TK3(n) + m(n)$ .

Define now:

$$x_1 = (1 - \gamma)m, \tag{A15}$$

$$x_2 = (1 - \gamma) \tag{A16}$$

$$x_3 = \alpha\gamma, \tag{A17}$$

$$\sigma_{TK3}^2 = (1 + 2\gamma^2 - 2\gamma)\sigma_T^2. \quad (A18)$$

From this it follows that:

$$\gamma = (1 - x_2), \quad (A19)$$

$$m = \frac{x_1}{1 - \gamma} = \frac{x_1}{x_2}, \quad (A20)$$

$$\alpha = \frac{x_3}{\gamma} = \frac{x_3}{1 - x_2}, \quad (A21)$$

$$\sigma_T^2 = \sigma_{TK3}^2 / (1 + 2\gamma^2 - 2\gamma). \quad (A22)$$

In this model it is essential to assume that  $mean(e)=0$  and that  $mean(s)=mean(r)=T_0$ . To ensure that this holds we subtract the empirical mean of  $e$  from  $e$  before we start.

Now we can write the Joint ADAM ( $\alpha$ ) with the new parameterization as:

$$b = \begin{bmatrix} r'(3) \\ \vdots \\ r'(n+1) \end{bmatrix} = A \times x + z$$

$$= \begin{bmatrix} s'(2) - s'(1) & s'(2) - e'(2) & -e'(2) \\ \vdots & \vdots & \vdots \\ s'(n) - s'(n-1) & s'(n) - e'(n) & -e'(n) \end{bmatrix} \begin{bmatrix} x_1 \\ x_2 \\ x_3 \end{bmatrix} + \begin{bmatrix} z(2) \\ \vdots \\ z(n) \end{bmatrix}$$

In this equation we assume that we reduced the empirical mean from the vectors so that:  $mean(e')=mean(s')=mean(r')=0$ .

We can solve this model using the bGLS method, and then project back to original parameters space using Eqs. (A19)–(A22).

Note that in the bGLS method we use the assumption that:  $\sigma_T^2 > \sigma_M^2$ . This assumption is essential because otherwise parameter interdependence deteriorate the estimation accuracy (Jacoby et al., in press).

However, for this model, this assumption is not enough to avoid parameter interdependence. This causes relatively large estimation errors for the parameter  $\alpha$ . The negative effect of this problem can be reduced using further assumptions on the parameter space, similar to the assumption that  $\sigma_T^2 > \sigma_M^2$  used in the original bGLS method (e.g Repp et al., 2012). The idea is to restrict the possible  $\alpha$  values to a smaller range for example:

$$L < \alpha < H,$$

where  $L = -0.8$  and  $H = -0.1$ . This range is determined based on simulations. This, therefore, implies that:

$$L < \frac{x_3}{1 - x_2} < H.$$

Within the bGLS iterations, if  $x_3/(1 - x_2) < L$  or  $x_3/(1 - x_2) > H$ , we change  $x_3$  so that the result is in the right range. This of course imposes further restrictions on the parameters that the estimation method can detect, but significantly reduces the estimation error variance.

### Joint ADAM ( $\beta$ )

ADAPTATION module:

$$t_{adap_{n+1}} = t_n + T_n - (\alpha + \beta) \times asyn_n + TK1_n$$

$$T_{n+1} = T_n - \beta \times asyn_n$$

We assume [ $\alpha=0$ ].

ANTICIPATION module:

$$IOI_{pred_{n+1}} = Int_{n+1} = a + b \times (n + 1)$$

$$IOI_{track_{n+1}} = tone_n - tone_{n-1}$$

$$tone_{anti_{n+1}} = tone_n + (m \times IOI_{pred_{n+1}} + (1 - m) \times IOI_{track_{n+1}}) + TK2_n$$

LINK module:

$$asyn_{joint} = t_{adap_{n+1}} - tone_{anti_{n+1}}$$

$$t_{n+1} = t_{adap_{n+1}} - ((1 - \gamma) \times asyn_{joint}) + M_{noise}$$

Using the new notation, we write:

ADAPTATION module:

$$t_{adap_{n+1}} = R(n) + T_n - (\alpha + \beta) \times e(n) + TK1(n), \quad (A23)$$

$$T_n = T_0 - \beta \times \sum_{N=1}^{n-1} e(N) \quad (A24)$$

ANTICIPATION module:

$$IOI_{pred_{n+1}} = Int_{n+1} = a + b \times (n + 1) = 2s(n) - s(n-1) \quad (A25)$$

$$IOI_{track_{n+1}} = tone_n - tone_{n-1} = s(n) \quad (A26)$$

$$tone_{anti_{n+1}} = S(n) + (m \times (2s(n) - s(n-1)) + (1 - m) \times s(n)) + TK2(n)$$

$$= S(n) + (m + 1)s(n) - m \times s(n-1) + TK2(n) \quad (A27)$$

joint module:

$$asyn_{joint} = t_{adap_{n+1}} - tone_{anti_{n+1}}$$

$$= [R(n) + T_n - (\alpha + \beta) \times e(n) + TK1(n)] - [S(n) + (m + 1)s(n) - m \times s(n-1) + TK2(n)]$$

$$= (1 - \alpha)e(n) + T_n - \beta e(n) - (m + 1)s(n) + m \times s(n-1) + TK1(n) - TK2(n)$$

$$= (1 - \alpha)e(n) + T_0 - \beta \times \sum_{N=1}^{n-1} e(N) - \beta e(n) - (m + 1)s(n) + m \times s(n-1) + TK1(n) - TK2(n) \quad (A28)$$

$$t_{n+1} = t_{adap_{n+1}} - ((1 - \gamma) \times asyn_{joint}) + M_{noise}$$

$$= R(n) + T_0 - \beta \times \sum_{N=1}^{n-1} e(N) - (\alpha + \beta) \times e(n) + TK1(n) + M(n) - M(n-1)$$

$$- ((1 - \gamma) \times (1 - \alpha)e(n) + T_0 - \beta \times \sum_{N=1}^{n-1} e(N) - \beta e(n) - (m + 1)s(n) + m \times s(n-1) + TK1(n) - TK2(n)) \quad (A29)$$

This can be written as:

$$r(n + 1) + (-\gamma)T_0 = (1 - \gamma)m \times [s(n) - s(n-1)] + (1 - \gamma) [s(n) - e(n)] + (\alpha\gamma)(-e(n)) - \gamma\beta \sum_{N=1}^n e(N) + z(n), \quad (A30)$$

where  $z(n) = [\gamma TK1(n) + (1 - \gamma)TK2(n) + m(n)] = TK3(n) + m(n)$ .

Define now

$$x_1 = (1 - \gamma)m, \quad (A31)$$

$$x_2 = (1 - \gamma), \quad (A32)$$

$$x_3 = \beta\gamma, \quad (A33)$$

$$\sigma_{TK3}^2 = (1 + 2\gamma^2 - 2\gamma)\sigma_T^2. \quad (A34)$$

From this it follows that:

$$\gamma = (1 - x_2), \quad (A35)$$

$$m = \frac{x_1}{1 - \gamma} = \frac{x_1}{x_2}, \quad (A36)$$

$$\beta = \frac{x_3}{\gamma} = \frac{x_3}{1 - x_2}, \quad (A37)$$

$$\sigma_T^2 = \frac{\sigma_{TK3}^2}{(1 + 2\gamma^2 - 2\gamma)} \tag{A38}$$

In this model it is essential to assume that  $mean(e)=0$  and that  $mean(s)=mean(r)=T_0$ . To ensure that this holds we reduce the empirical mean of  $e$  from  $e$  before we start.

Now we can write the Joint ADAM ( $\beta$ ) with the new parameterization as:

$$b = \begin{bmatrix} r'(3) \\ \vdots \\ r'(n+1) \end{bmatrix} = A \times x + z$$

$$= \begin{bmatrix} s'(2)-s'(1) & s'(2)-e'(2) & -\sum_{n=1}^2 e'(n) \\ \vdots & \vdots & \vdots \\ s'(n)-s'(n-1) & s'(n)-e'(n) & -\sum_{n=1}^n e'(n) \end{bmatrix} \begin{bmatrix} x_1 \\ x_2 \\ x_3 \end{bmatrix}$$

$$+ \begin{bmatrix} z(2) \\ \vdots \\ z(n) \end{bmatrix}$$

In this equation we assume that we reduced the empirical mean from the vectors so that:  $mean(e')=mean(s')=mean(r')=0$ .

We can solve this model using the bGLS method, and then project back to original parameters space using Eqs. (A35)–(A38). Unfortunately this gives relatively large estimation error for the parameter  $\beta$  (as was the case with  $\alpha$ ).

Again, this problem is generated because of the parameter interdependence of the model. The negative effect of this problem can be reduced by restricting the possible  $\beta$  values to a smaller range for example:

$$L < \beta < H,$$

where  $L=0$  and  $H=1$

This, therefore, implies that:

$$L < \frac{x_3}{1-x_2} < H$$

Within the bGLS iterations, if  $x_3/(1-x_2) < L$  or  $x_3/(1-x_2) > H$ , we change  $x_3$  so that the result is in the right range. Furthermore, we restrict  $m$  to the same range.

$$L < m < H$$

$$L < x_1/x_2 < H$$

If  $x_2$  is positive:

$$x_2 L < x_1 < x_2 H$$

This of course imposes further restrictions on the parameters that the estimation method can detect but significantly reduces the estimation error variance.

Note that like any bGLS estimates we also assume that  $\sigma_T^2 > \sigma_M^2$ .

### Hybrid ADAM

Interval prediction: Interval tracking:

$$Int_{n+1} = a + b \times (n + 1) \quad TRACK_{n+1} = tone_n - tone_{n-1}$$

$$PRED_{n+1} = tone'_{n+1} - t_n$$

$$tone'_{n+1} = tone_n + Int_{n+1}$$

$$t_{n+1} = t_n + (m \times PRED_{n+1} + (1-m) \times TRACK_{n+1}) - \alpha \times asyn_n + TK_n + M_n - M_{n-1}$$

Using the new notation we write:

$$PRED_{n+1} = tone'_{n+1} - t_n = S(n) + 2s(n) - s(n-1) - R(n) = 2s(n) - s(n-1) - e(n) \tag{A39}$$

$$tone'_{n+1} = tone_n + Int_{n+1} = S(n) + 2s(n) - s(n-1) \tag{A40}$$

$$TRACK_{n+1} = tone_n - tone_{n-1} = S(n) - S(n-1) = s_n \tag{A41}$$

$$t_{n+1} = t_n + (m \times PRED_{n+1} + (1-m) \times TRACK_{n+1}) - \alpha \times asyn_n + noise$$

$$= R(n) + (m \times (2s(n) - s(n-1) - e(n)) + (1-m) \times s(n)) - \alpha \times e(n) + z(n) \tag{A42}$$

This can be written as:

$$r(n+1) = m [s(n) - s(n-1) - e(n)] + \alpha(-e(n)) + s(n) + z(n) \tag{A43}$$

The Hybrid model can be written therefore in matrix notation as:

$$b = \begin{bmatrix} r(3) - s(2) \\ \vdots \\ r(n+1) - s(n) \end{bmatrix} = A \times x + z$$

$$= \begin{bmatrix} s(2) - s(1) - e(1) & -e(2) \\ \vdots & \vdots \\ s(n) - s(n-1) - e(n) & -e(n) \end{bmatrix} \begin{bmatrix} m \\ \alpha \end{bmatrix} + \begin{bmatrix} z(2) \\ \vdots \\ z(n) \end{bmatrix}$$

This formulation can be again solved with the bGLS method.

For one block of the experiment, the method provided unbiased estimates for large values of  $m$ . For small values of  $m$  more bias is observed in the  $\alpha$  parameters and the estimation error is relatively large. We increased the accuracy of estimates by averaging over the 15 repetitions for each pattern.

### REFERENCES

Brockwell, P.J., Davis, R.A., 2009. *Time Series: Theory and Methods*. Springer, New York, NY.

Butz, M.V., Sigaud, O., Gérard, P., 2003. Anticipatory behavior: exploiting knowledge about the future to improve current behavior. In: Butz, M.V., Sigaud, O., Gérard, P. (Eds.), *Anticipatory behavior in adaptive learning systems*. Foundations, theories, and systems. Springer, Berlin, Germany, pp. 1–10.

Dean, R.T., Bailes, F., 2010. Time series analysis as a method to examine acoustical influences on real-time perception of music. *Empir. Musicol. Rev.* 5, 152–175.

Drake, C., Penel, A., Bigand, E., 2000. Tapping in time with mechanically and expressively performed music. *Music Percept.* 18, 1–23.

Friberg, A., Sundberg, J., 1995. Time discrimination in a monotonic, isochronous sequence. *J. Acoust. Soc. Am.* 98, 2524–2531.

Grush, R., 2004. The emulation theory of representation: motor control, imagery, and perception. *Behav. Brain. Sci.* 27, 377–442.

Jacoby, N., Repp, B.H., 2012. A general linear framework for the comparison and evaluation of models of sensorimotor synchronization. *Biol. Cybern.* 106, 135–154.

Jacoby, N., Repp, B.H., Ahissar, M., Tishby, N., & Keller, P.E. (in press). Parameter estimation of linear sensorimotor synchronization models: Phase correction, period correction and ensemble synchronization. *Timing & Time Perception*.

- Keller, P.E., Knoblich, G., Repp, B.H., 2007. Pianists duet better when they play with themselves: on the possible role of action simulation in synchronization. *Conscious. Cogn.* 16, 102–111.
- Keller, P.E., 2008. Joint action in music performance. In: Morganti, F., Carassa, A., Riva, G. (Eds.), *Enacting Intersubjectivity: A Cognitive and Social Perspective to the Study of Interactions*. IOS Press, Amsterdam, The Netherlands, pp. 205–221.
- Keller, P.E., 2014. Ensemble performance: interpersonal alignment of musical expression. In: Fabian, D., Timmers, R., Schubert, E. (Eds.), *Expressiveness in Music Performance: Empirical Approaches Across Styles and Cultures*. Oxford University Press, Oxford, UK, pp. 260–282.
- Keller, P.E., Novembre, G., Hove, M.J., 2014. Rhythm in joint action: psychological and neurophysiological mechanisms for real-time interpersonal coordination. *Philos. Trans. R. Soc. B* 369, 1658.
- Keller, P.E., Novembre, G., & Loehr, J. (in press). Musical ensemble performance: Representing self, other, and joint action outcomes. In E.S. Cross & S.S. Obhi (Eds.), *Shared representations: Sensorimotor foundations of social life*. Cambridge: Cambridge University Press.
- Keller, P.E., 2012. Mental imagery in music performance: underlying mechanisms and potential benefits. *Ann. NY Acad. Sci.* 1252, 206–213.
- Launay, J., Dean, R.T., Bailes, F., 2013. Evidence for multiple strategies in off-beat tapping with anisochronous stimuli. *Psychol. Res.* <http://dx.doi.org/10.1007/s00426-013-0513-9> [Epub ahead of print].
- Madison, G., Merker, B., 2005. Timing of action during and after synchronization with linearly changing intervals. *Music Percept.* 22, 441–459.
- Mates, J., 1994a. A model of synchronization of motor acts to a stimulus sequence: I. Timing and error corrections. *Biol. Cybern.* 70, 463–473.
- Mates, J., 1994b. A model of synchronization of motor acts to a stimulus sequence: II. Stability analysis, error estimation and simulations. *Biol. Cybern.* 70, 475–484.
- Michon, J.A., 1967. *Timing in Temporal Tracking*. Van Gorcum, Assen, The Netherlands.
- Mills, P.F., van der Steen, M.C., Schultz, B.G., & Keller, P.E. (in press). Individual differences in temporal anticipation and adaptation during sensorimotor synchronization. *Timing & Time Perception*.
- Palmer, C., 1997. Music performance. *Annu. Rev. Psychol.* 48, 138–155.
- Pecenka, N., Keller, P.E., 2009. Auditory pitch imagery and its relationship to musical synchronization. *Ann. NY Acad. Sci.* 1169, 282–286.
- Pecenka, N., Keller, P.E., 2011. The role of temporal prediction abilities in interpersonal sensorimotor synchronization. *Exp. Brain Res.* 211, 505–515.
- Pecenka, N., Engel, A., Keller, P.E., 2013. Neural correlates of auditory temporal predictions during sensorimotor synchronization. *Front. Hum. Neurosci.* 7, 380, <http://dx.doi.org/10.3389/fnhum.2013.00380>.
- Pickering, M., Garrod, S., 2013. An integrated theory of language production and comprehension. *Behav. Brain Sci.* 36, 329–347.
- Pickering, M.J., Garrod, S., 2014. Self-, other-, and joint monitoring using forward models. *Front. Hum. Neurosci.* 8, 132, <http://dx.doi.org/10.3389/fnhum.2014.00132>.
- Phillips-Silver, J., Keller, P.E., 2012. Searching for roots of entrainment and joint action in early musical interactions. *Front. Hum. Neurosci.* 6, 26, <http://dx.doi.org/10.3389/fnhum.2012.00026>.
- Rankin, S.K., Large, E.W., Fink, P.W., 2009. Fractal tempo fluctuation and pulse prediction. *Music Percept.* 26, 401–413.
- Repp, B.H., 1998. A microcosm of musical expression. I. Quantitative analysis of pianists' timing in the initial measures of Chopin's Etude in E major. *J. Acoust. Soc. Am.* 104, 1085–1100.
- Repp, B.H., 2001a. Phase correction, phase resetting, and phase shifts after subliminal timing perturbations in sensorimotor synchronization. *J. Exp. Psychol. Hum. Percept. Perform.* 27, 600–621.
- Repp, B.H., 2001b. Processes underlying adaptation to tempo changes in sensorimotor synchronization. *Hum. Mov. Sci.* 20, 277–312.
- Repp, B.H., 2002a. The embodiment of musical structure: effects of musical context on sensorimotor synchronization with complex timing patterns. In: Prinz, W., Hommel, B. (Eds.), *Common Mechanisms in Perception and Action: Attention And Performance XIX*. Oxford University Press, Oxford, UK, pp. 245–265.
- Repp, B.H., 2002b. Automaticity and voluntary control of phase correction following event onset shifts in sensorimotor synchronization. *J. Exp. Psychol. Hum. Percept. Perform.* 28, 410–430.
- Repp, B.H., 2005. Sensorimotor synchronization: a review of the tapping literature. *Psychon. Bull. Rev.* 12, 969–992.
- Repp, B.H., 2006. Musical synchronization. In: Altenmüller, E., Wiesendanger, M., Kesselring, J. (Eds.), *Music, Motor Control, and the Brain*. Oxford University Press, Oxford, UK, pp. 55–76.
- Repp, B.H., 2008. Metrical subdivision results in subjective slowing of the beat. *Music Percept.* 26, 19–39.
- Repp, B.H., Bruttomesso, M., 2009. A filled duration illusion in music: effects of metrical subdivision on the perception and production of beat tempo. *Adv. Cogn. Psychol.* 5, 114–134.
- Repp, B.H., Keller, P.E., 2004. Adaptation to tempo changes in sensorimotor synchronization: effects of intention, attention, and awareness. *Q. J. Exp. Psychol.* 57A, 499–521.
- Repp, B.H., Keller, P.E., 2008. Sensorimotor synchronization with adaptively timed sequences. *Hum. Mov. Sci.* 27, 423–456.
- Repp, B.H., Keller, P.E., Jacoby, N., 2012. Quantifying phase correction in sensorimotor synchronization: empirical comparison of three paradigms. *Acta Psychol.* 139, 281–290.
- Schulze, H.-H., Cordes, A., Vorberg, D., 2005. Keeping synchrony while tempo changes: accelerando and ritardando. *Music Percept.* 22, 461–477.
- Schmidt, R.A., 1968. Anticipation and timing in human motor performance. *Psychol. Bull.* 70, 631–646.
- Sebanz, N., Knoblich, G., 2009. Prediction in joint action: what, when, and where. *Top. Cogn. Sci.* 1, 353–367.
- Semjen, A., Vorberg, D., Schulze, H.-H., 1998. Getting synchronized with the metronome: comparisons between phase and period correction. *Psychol. Res.* 61, 44–55.
- Thaut, M.H., Miller, R.A., Schauer, L.M., 1998a. Multiple synchronization strategies in rhythmic sensorimotor tasks: phase vs period correction. *Biol. Cybern.* 79, 241–250.
- Thaut, M.H., Tian, B., Azimi-Sadjadi, 1998b. Rhythmic finger tapping to cosine-wave modulated metronome sequences: evidence of subliminal entrainment. *Hum. Mov. Sci.* 17, 839–863.
- Thaut, M.H., Stephan, K.M., Wunderlich, G., Schicks, W., Tellmann, L., Herzog, H., McIntosh, G.C., Seitz, R.J., Hömber, V., 2009. Distinct cortico-cerebellar activations in rhythmic auditory motor synchronization. *Cortex* 45, 44–53.
- van der Steen, M.C., Keller, P.E., 2013. The Adaptation and Anticipation Model (ADAM) of sensorimotor synchronization. *Front. Hum. Neurosci.* 7, 253, <http://dx.doi.org/10.3389/fnhum.2013.00253>.
- van der Steen, M.C., Schwartze, M., Kotz, S.A., & Keller, P.E. (in press). Modeling effects of cerebellar and basal ganglia lesions on adaptation and anticipation during sensorimotor synchronization. *Annals of the New York Academy of Sciences*.
- Vorberg, D., Wing, A., 1996. Modeling variability and dependence in timing. In: Heuer, H., Keele, S.W. (Eds.), *Handbook of*

- Perception and Action, vol. 2. Academic Press, London, UK, pp. 181–262.
- Vorberg, D., Schulze, H.-H., 2002. A two-level timing model for synchronization. *J. Math. Psychol.* 46, 56–87.
- Wing, A.M., 1980. The long and short of timing in response sequences. In: Stelmach, G.E., Requin, J. (Eds.), *Tutorials in Motor Behavior*. North-Holland, Amsterdam, pp. 469–486.
- Wing, A.M., Kristofferson, A.B., 1973. Response delays and the timing of discrete motor responses. *Percept. Psychophys.* 14, 5–12.
- Wing, A.M., Endo, S., Bradbury, A., Vorberg, D., 2014. Optimal feedback correction in string quartet synchronization. *J. R. Soc. Interface* 11, 20131125, <http://dx.doi.org/10.1098/rsif.2013.1125>.
- Wilson, M., Knoblich, G., 2005. The case of motor involvement in perceiving conspecifics. *Psychol. Bull.* 131, 460–473.
- Wolpert, D.M., Doya, K., Kawato, M., 2003. A unifying computational framework for motor control and social interaction. *Philos. Trans. Roy. Soc. B* 358, 593–602.
- Wolpert, D.M., Kawato, M., 1998. Multiple paired forward and inverse models for motor control. *Neural Netw.* 11, 1317–1329.